Original Article

An unprecedented bloom of *Lingulodinium polyedra* on the French Atlantic coast during summer 2021

Kenneth Neil Mertens [a],[*], Michael Retho [b], Soazig Manach [b], Maria Laura Zoffoli [c], Anne Doner [a], Mathilde Schapira [d], Gwenael Bilien [a], Véronique Séchet [e], Thomas Lacour [e], Elise Robert [f], Audrey Duval [a], Aouregan Terre-Terrillon [a], Amélie Derrien [a], Pierre Gernez [g]

[a] *Ifremer, LITTORAL, F-29900 Concarneau, France*
[b] *Ifremer, LITTORAL, F-56100, Lorient, France*
[c] *Consiglio Nazionale delle Ricerche, Istituto di Scienze Marine (CNR-ISMAR), 00133, Rome, Italy*
[d] *Ifremer, LITTORAL, F-44300, Nantes, France*
[e] *Ifremer, PHYTOX, Laboratoire PHYSALG, F-44000 Nantes, France*
[f] *Ifremer, PHYTOX, Laboratoire GENALG, F-44000 Nantes, France*
[g] *Nantes Université, Institut des Substances et Organismes de la Mer, ISOMer, UR 2160, F-44000 Nantes, France*

ARTICLE INFO

ABSTRACT

At the end of July 2021, a bloom of *Lingulodinium polyedra* developed along the French Atlantic coast and lasted six weeks. The REPHY monitoring network and the citizen participation project PHENOMER contributed to its observation. A maximum concentration of 3,600,000 cells/L was reached on the 6th of September, a level never recorded on French coastlines. Satellite observation confirmed that the bloom reached its highest abundance and spatial extension early September, covering about 3200 km^2 on the 4th of September. Cultures were established, and morphology and ITS-LSU sequencing identified the species as *L. polyedra*. The thecae displayed the characteristic tabulation and sometimes a ventral pore. The pigment composition of the bloom was similar to that of cultured *L. polyedra*, confirming that phytoplankton biomass was dominated by this species. The bloom was preceded by *Leptocylindrus* sp., developed over *Lepidodinium chlorophorum*, and was succeeded by elevated *Noctiluca scintillans* concentrations. Afterwards, relatively high abundance of *Alexandrium tamarense* were observed in the embayment where the bloom started. Unusually high precipitation during mid-July increased river discharges from the Loire and Vilaine rivers, which likely fueled phytoplankton growth by providing nutrients. Water masses with high numbers of dinoflagellates were characterized by high sea surface temperature and thermohaline stratification. The wind was low during the bloom development, before drifting it offshore. Cysts were observed in the plankton towards the end of the bloom, with concentrations up to 30,000 cysts/L and relative abundances up to 99%. The bloom deposited a seed bank, with cyst concentrations up to 100,000 cysts/g dried sediment, particularly in fine-grained sediments. The bloom caused hypoxia events, and concentrations of yessotoxins up to 747 μg/kg were recorded in mussels, below the safety threshold of 3,750 μg/kg. Oysters, clams and cockles also were contaminated with yessotoxins, but at lower concentrations. The established cultures did not produce yessotoxins at detectable levels, although yessotoxins were detected in the sediment. The unusual environmental summertime conditions that triggered the bloom, as well as the establishment of considerable seed banks, provide important findings to understand future harmful algal blooms along the French coastline.

1. Introduction and aims

Dinoflagellates are a group of microorganisms that can produce blooms that can be harmful and are called harmful algal blooms (HABs). Blooms are expanding and intensifying globally (Dai et al., 2023), and some of these blooms can cause surface seawater discoloration (i.e., green, red, brown) that can be detected using satellite remote sensing (e. g. Gernez et al., 2023, and references therein). Such massive blooms alter the appearance of coastal waters (Siano et al., 2020) and the remineralisation of the high volume of biomass produced during these

phenomena may create hypoxic/anoxic conditions that are deleterious for marine aquaculture and ecosystems (Sournia et al., 1992). For example, green seawater discolorations caused by the marine dinoflagellate *Lepidodinium chlorophorum* have frequently been observed along Southern Brittany (NE Atlantic, France; Roux et al., 2022, 2023). Other HAB species produce toxins which can accumulate in shellfish and other marine organisms. Most toxigenic dinoflagellates belong to the order Gonyaulacales, either to planktonic genera such as *Alexandrium, Lingulodinium,* and *Protoceratium,* or benthic ones such as *Gambierdiscus, Ostreopsis* and *Coolia* (Lassus et al., 2016; Table 1 on p. 16). The planktonic genera *Gonyaulax, Protoceratium* and *Lingulodinium* produce yessotoxins (YTXs; Paz et al., 2008) and these can be potentially produced by *Pentaplacodinium* (Mertens et al., 2018; K.N. 2023). YTXs are polycyclic ether-compounds that are considered to be potent cytotoxins, this caused the European Authorities to establish a maximum permitted level in shellfish, which currently is as high as 3.75 mg YTX equivalents/kg (Regulation 786/EC/2013; Rubini et al., 2021).

One such YTX-producing species, *Lingulodinium polyedra* (F. Stein) J. D. Dodge 1989 is an autotrophic, thecate dinoflagellate that recently was restudied from its type locality, Kiel Bight in Germany (Tillmann et al., 2021). Blooms of this species have been related to enhanced nutrient levels that might be supplied by coastal runoff, upwelling or anthropogenic inputs (Lewis and Hallett, 1997, p. 136), and can cause brown water discoloration (e.g. Peña-Manjarrez et al., 2005, p. 1384). In Europe, blooms are known to occur mostly in southern European waters, and have since long been recorded from the Adriatic, specifically in Kaštela Bay (e.g., Marasović and Vukadin, 1982), around Spain (e.g., Margalef, 1956, Caballero et al., 2020) and Portugal (Amorim et al., 2000). A most recent bloom was observed in Odessa Bay (Ukraine, Black Sea) in 2020, with highest ever recorded concentrations up to 56.1 million cells/L (Terenko and Krakhmalny, 2021). Outside Europe, blooms have repeatedly been reported off California (e.g., Eppley and Harrison, 1975; Kahru et al., 2021) and along the Southern (Pitcher et al., 2019) and Northern African coast (e.g., Bennouna et al., 2002, Frehi et al., 2007). For several *L. polyedra* events, satellite remote sensing made it possible to accurately document the bloom's spatial and temporal variability, thus usefully complementing field sampling (Caballero et al., 2020; Kahru et al., 2021).

Production of YTXs by *L. polyedra* has been demonstrated from cultures from NW Spain (Paz et al., 2004), California (Armstrong and Kudela, 2006) and the U.K. (Stobo et al., 2003). Elevated YTXs from mussels from the North Adriatic Sea and the Black Sea have been attributed to *L. polyedra* blooms (Tubaro et al., 1998; Morton et al., 2007; Rubini et al., 2021), amongst other reports. Mortalities of fish and other organisms have, however, more often been attributed to high bloom concentrations leading to anoxia (Lewis and Hallett, 1997, p. 110 and references therein).

L. polyedra is a well-known cyst-producer that has been related to the fossil defined species *Lingulodinium machaerophorum* (e.g. Mertens et al.,

2009a). The process of cyst-formation has been described in detail by Kokinos and Anderson (1995). Cysts are produced at the end of the bloom (Amorim et al., 2000) and form seed banks that accumulate preferentially in fine-grained sediments (Lewis, 1988). In general, after the encystment in autumn and a mandatory dormancy period in winter, excystment occurs in spring (Lewis and Hallett, 1997, fig. 31). Cysts of *L. polyedra* are widely distributed in temperate to equatorial regions, with highest relative abundances near upwelling regions or below river discharge plumes (Zonneveld et al., 2013).

In France, the plankton is monitored through the REPHY network (REPHY, 2022), and toxins in shellfish through the REPHYTOX network (REPHYTOX, 2022). In the French Atlantic, HABs are typically related to *Dinophysis* spp., *Alexandrium* and *Pseudo-nitzschia* (Belin et al., 2021). Cells of *L. polyedra* have been observed in the French Atlantic since 1964 (e.g. Paulmier, 1965, 1994). One oyster mortality event during summer 1964 was associated with elevated concentrations of this species in the Auray Estuary (Paulmier, 1972). Cysts have been studied rather rarely along the French Atlantic coasts. Cysts of *L. polyedra* were first recorded in 1989 and 1990 in surface sediments from Vilaine Bay by An et al. (1992), whom recorded maximum concentrations of about 110 cysts/g sediment, although none were recorded in surface sediments from Vilaine Bay sampled in 1986 and 1987 by Larrazabal et al. (1990). However, palynological studies show that the cysts have been present for thousands of years along the French Atlantic coast (e.g. Lambert et al., 2020).

In this study, we report an unprecedented summer bloom of *L. polyedra* from the French Atlantic using in situ and satellite observations. We identify the species morpho-molecularly, identify its pigments and examine its toxicity. We investigate the potential triggers for the bloom, and discuss its decline. The imprint of a seed bank is investigated by quantifying the cysts in surface sediments.

2. Material and methods

2.1. Observation area and sampling stations

On the French Atlantic Ocean, the Northern Bay of Biscay, and more precisely the coastal zone in southern Brittany (France), is directly influenced by the Vilaine and Loire Rivers, which have a respective 70 and 850 m^3/s mean annual flow (Lazure et al., 2009). Both rivers, and especially the Loire, are the main nutrient sources in the northern Bay of Biscay and play a major role in the eutrophication of coastal waters in southern Brittany (Guillaud et al., 2008; Ménesguen et al., 2018, 2019; Ratmaya et al., 2019). The location and extent of both rivers plumes vary according to the flow of rivers, tidal currents and winds. In winter, the Loire river plume can be oriented towards the northwest along the coast, and in periods of very high flow, the plume extends seaward (Ménesguen and Dussauze, 2015; Ménesguen et al., 2018). The Vilaine river plume generally spreads throughout the Bay before moving

Table 1

Sampling localities for surface sediment samples obtained for cyst counts, with geographic coordinates, water depth, sampling date and sampling device.

Sample name	Longitude	Latitude	Water depth (m)	Sampling date	Sampling device
Doëlan	−3.60333	47.77671	0.0	7-Apr-22	By hand
Lorient	−3.36556	47.71833	12.0	1-Mar-22	Petite Ponar Grab
Men er Roué	−3.09375	47.53477	9.0	15-Mar-22	Petite Ponar Grab
Anse de Pen Men	−2.83427	47.61439	0.0	29-Mar-22	By hand
Pénerf	−2.64783	47.50798	6.3	14-Mar-22	Petite Ponar Grab
Port Mahé	−2.48467	47.43435	5.4	14-Mar-22	Petite Ponar Grab
Marescelé	−2.50060	47.46197	5.0	14-Mar-22	Petite Ponar Grab
Estuaire Vilaine	−2.52568	47.50985	4.2	14-Mar-22	Petite Ponar Grab
Ouest Loscolo	−2.53827	47.45759	10.0	14-Mar-22	Petite Ponar Grab
Nord Dumet	−2.65678	47.46020	14.5	14-Mar-22	Petite Ponar Grab
Le Croisic	−2.53412	47.27345	26.0	28-Mar-22	Petite Ponar Grab
Pornichet	−2.34646	47.25781	3.0	23-Feb-22	Petite Ponar Grab
La Coupelassse	−2.02635	47.01644	0.0	4-Apr-22	By hand
St Gildas	−2.32037	47.17267	24.0	29-Mar-22	Petite Ponar Grab

westward (Chapelle et al., 1994). The water circulation within the Vilaine Bay is characterized by low tidal and residual currents, and is mainly driven by tide, wind and river flow (Lazure and Salomon, 1991; Lazure and Jegou, 1998). The water residence time in the bay varies from 10 to 20 days depending on the season and is generally longer during calm periods (Chapelle et al., 1994). Haline stratification is high from February to June in response to high river runoff and relatively low vertical mixing, whereas thermal stratification occurs between May and mid-September (Puillat et al., 2004).

Data from REPHY (Observation and Surveillance Network for Phytoplankton and hydrology in coastal waters; Belin et al., 2021; REPHY, 2022) stations and PHENOMER observations (a citizen monitoring program focused on water discoloration observations, Siano et al., 2020) were used to describe the bloom of *L. polyedra* and the environmental conditions (Fig. 1).

2.2. Environmental data

Air temperature data were retrieved from the weather station Vannes-Séné (2.7141°W; 47.6045°N) and daily wind data were retrieved from the weather station Belle Ile – Le Talut (3.2181°W; 47.2942°N) using Météo France observation network (https://donneespubliques.meteofrance.fr/). River discharge data were extracted from the French hydrological database (http://www.hydro.eaufrance.fr/). Daily discharge data were available at the Montjean-sur-Loire gaging station for the Loire River and at the Rieux gaging station for

the Vilaine River. Sea water temperature, salinity, and inorganic nutrients data were provided by the REPHY and the research project LEPIDO-PEN. Data from three stations were analyzed: "Ouest Loscolo" (OL) and "Nord Dumet" (ND) located off the Vilaine estuary, and "Basse Michaud" (BM) located off the Loire estuary (Fig. 1). Samples were collected at these stations fortnightly at high tide (+/- 2 h). Vertical profiles of seawater temperature, salinity, turbidity (FNU) and in vivo fluorescence (FFU) were performed with a multi-parameter probe type MP6 (NKE, Hennebont, France) from subsurface to the water-sediment interface (WSI). Water samples were collected using a 5 L Niskin bottle at two depths: subsurface (0–1 m) and 1 m above the WSI. Water samples aliquots were processed for (i) microphytoplankton identification and enumeration, (ii) chlorophyll *a* concentration ([Chl *a*] mg/m^3), and (iii) inorganic nutrients. Analytical procedure for plankton observations and counts are described in Section 2.2.

For Chl *a* concentrations, water samples (500–1000 ml) were filtered through glass fiber filters (GF/F 0.7 μm, 47 mm; Whatman, Maidstone, UK) and stored at −80 °c until analysis. Chl *a* was extracted in 10 mL of 90% acetone in the dark at 4 °C for 12 h and analysed by monochromatic spectrophotometry (Aminot and Kérouel, 2004).

For inorganic nutrients, 300 mL water samples were pre-filtered through 41 μm pore silk directly from the Niskin bottle. For dissolved silicate (i.e., DSi = Si(OH)$_4$) concentrations, water samples were filtered through 0.45 μm acetate cellulose membrane and stored at 4 °C until analysis. Water samples for the determination of dissolved inorganic nitrogen (i.e., DIN = NO$_3^-$ + NO$_2^-$ + NH$_4^+$) and phosphorus (i.e., DIP =
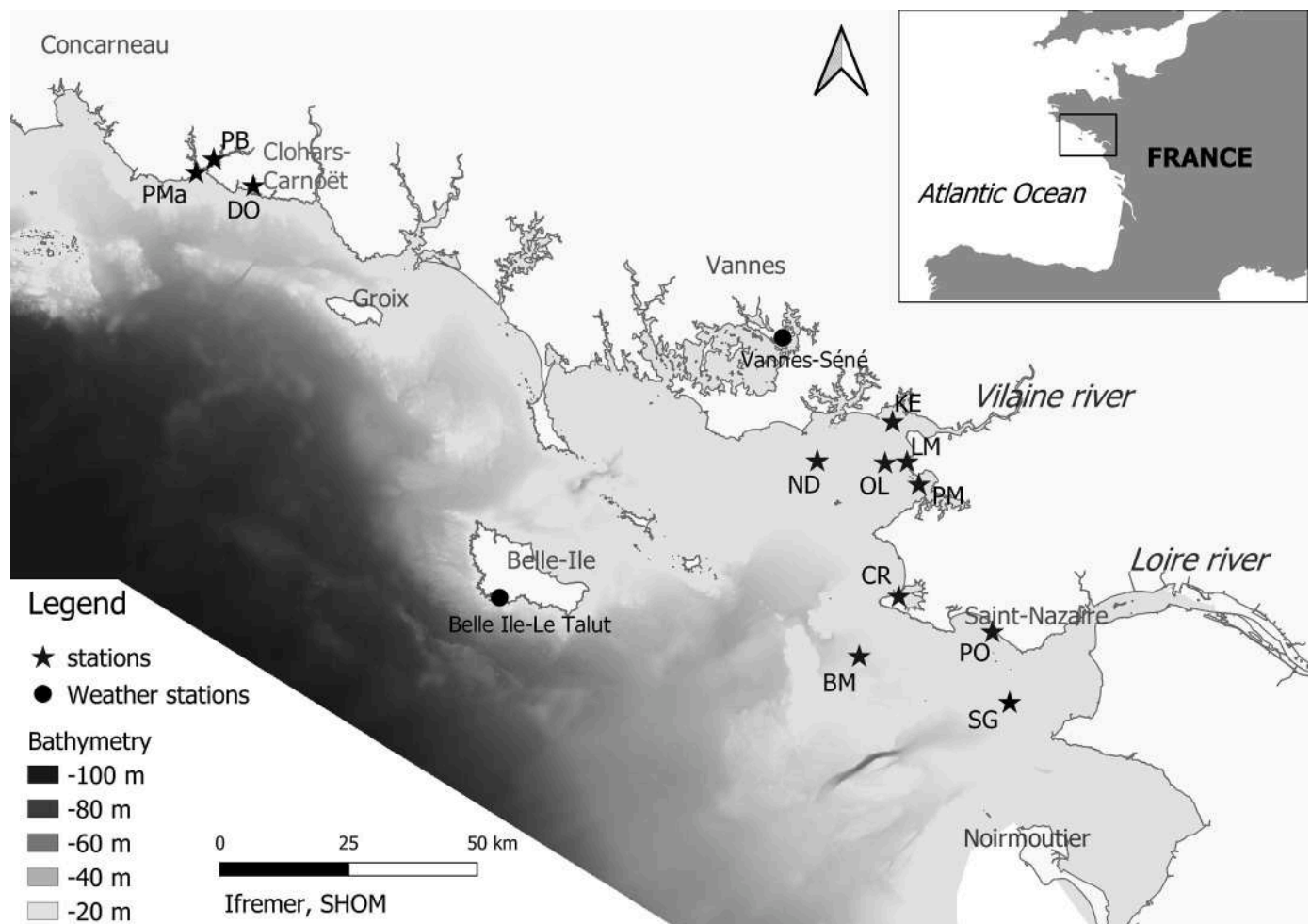

Fig. 1. Map of plankton and sediment sampling stations in southern Brittany as mentioned in the text. Major rivers and islands are indicated. BM = Basse Michaud, CR = Le Croisic, DO = Doëlan, KE = Kervoyal, LM = Le Maresclé, ND = Nord Dumet, OL = Ouest Loscolo, PB = Port Bélon, PM = Pont Mahé, PMa = Port Manec'h, PO = Pornichet Port, SG = Saint-Gildas, . Bathymetry is indicated by grayscale.

PO_4^{3-}) were stored directly at −20 °C. Samples were analysed using an AutoAnalyzer AA3 (SEAL Analytic, Mequon, WI, USA) following standard protocols (Aminot and Kérouel, 2007). The limits of quantification were 0.4 μM for DSi, 0.2 μM for $NO_3^- + NO_2^-$, and 0.05 μM for DIP, NH_4^+, and NO_2^-. Measurement uncertainty measurement are 12% for DSi, 10% for $NO_3^- + NO_2^-$, 15% for DIP, and 27% for NH_4^+.

In the Vilaine Bay, temperature and salinity at the ND station were also obtained from a high-frequency monitoring buoy, MOLIT, of the French national observation network COAST-HF. Since 2008, this instrumented buoy continuously measures physicochemical parameters in surface and bottom waters at hourly frequency (Retho et al., 2022). Furthermore, dissolved oxygen concentrations in bottom waters (1 m above the WSI) were acquired at the Pont Mahé (PM) station by an autonomous miniDOT sensor (PME, Vista, CA, USA) at high frequency (15 min).

2.2. Plankton observations and cell counts

L. polyedra distribution and abundance were assessed using REPHY (REPHY, 2022) and PHENOMER data. Cells of lugol-fixed *L. polyedra* were counted using an inverted microscope (Zeiss, Axio Observer). Samples were gently homogenized before settling in 10 mL sub-sample for > 12 h in counting chambers (Utermöhl, 1958; Hydro-Bios, Alenholz, Germany). The lower limit of quantification was 100 cells/L.

2.3. Satellite images

Satellite observations from the Ocean Land Colour Instrument (OLCI) on-board Sentinel-3 (S3) were used to study the bloom spatial and temporal variability. Since 2016, S3/OLCI acquires radiometric data in 21 spectral bands from 400 – 1020 nm with a revisit time < 2 days and a spatial resolution of 300 m. Images acquired between the 1st of July and 30th of September 2021 were downloaded from EUTMETSAT Earth Observation Portal (https://eoportal.eumetsat.int/). Level2 data, corresponding to water-leaving reflectance, were directly obtained from the portal. A total of 17 images with low cloud cover were found exploitable for the selected time window in the region of interest (latitude from 46.75°N – 48°N, and longitude from 1.5°W – 4°W). The concentration of Chl *a* in the first optical layer (typically < 5 m in coastal waters) was estimated by an algorithm specifically designed to retrieve [Chl *a*] over a wide range of variability, including extreme phytoplankton bloom conditions (Smith et al., 2018). Satellite-derived maps of [Chl *a*] were re-projected in an appropriate coordinate system (i.e., WGS 84 / UTM zone 30 N - EPSG: 32,630), and used to compute bloom areal extent. Satellite data processing and mapping were performed using the Matlab software.

2.4. Establishment of cultures

Living cells were isolated from plankton samples from Port Manec'h (strain IFR-CC-21–049), Doëlan (strain IFR-CC-21–048) and Le Croisic (strain IFR-LI-01LC) (PMa, DO, and CR, Fig. 1) using a micropipette, and placed in a single well of a 12-well plate, together with 500 μl L1 medium. Conditions for growth were 18 °C, 90 μEm^{-2}s^{-1} and a 12:12 h light:dark cycle.

2.5. Light microscopy and scanning electron microscopy observations

A lugol-fixed plankton sample acquired at station KE (Fig. 1) on the 2nd August was used to isolate cells and cysts of *L. polyedra*. For light microscopy, all measurements and light photomicrographs were obtained by K.N.M. using an Olympus BX41 with an Olympus DP72 camera, with 100X oil immersion objectives. All cyst and motile cell measurements in the species descriptions cite the minimum, average (in parentheses) and maximum values (μm), in that order.

For scanning electron microscopy (SEM), specimens were first isolated from the sample with a micropipette using an IX51 (Olympus, Tokyo, Japan) or an IM35 (Zeiss, Oberkochen, Germany) inverted microscope and transferred onto polycarbonate membrane filters (Millipore, Billerica, MA, USA; GTTP Isopore, 0.22 μm pore size), following a method proposed by Chomérat and Couté (2008). After 12 to 24 h of air-drying, the filters were affixed to aluminum stubs with adhesive tabs (Electron Microscopy Sciences, Hatfield, PA, USA). Subsequently, the mounted filters were sputter coated with gold using a 108auto Sputter coater (Cressington Scientific Instruments, UK). The samples were observed at the Station of Marine Biology of Concarneau with a Sigma 300 (Zeiss, Oberkochen, Germany) field-emission SEM equipped with a conventional Everhart–Thornley and in-lens detectors of secondary electrons at 1.5 and 5 kV. Digital images were saved in Tiff format (2048 × 1768 pixels). Photoshop Creative Suite 5 (CS5; Adobe, San Jose, CA, USA) software was used to remove the background while maintaining the integrity of the original image. labeling of tabulation follows a modified Kofoid system that recognizes homologs (Carbonell-Moore et al., 2021).

2.6. Sequencing of culture of L. polyedra

The cultures of *L. polyedra* established from Port Manec'h (IFR-CC-21–049) and Doëlan (IFR-CC-21–048) (PMa and DO, Fig. 1) were extracted with the PCRBIO Rapid Extract PCR Kit (PCR Biosystems Ltd, London, UK) which combines extraction and PCR. In a 1.5 ml tube, 1 ml of culture were taken and centrifuged for 3 min at 14,000 rpm. The supernatant was discarded to retain only the pellet. Then the manufacturer's instructions were followed, except for the step dilution where 190 μl of PCR grade dH$_2$O were added instead of 900 μl. The pair of primers used for the PCR is ITSFW (GTAGGTGAACCTGCGGAAGG) and D3B (TCGGAGGGAACCAGCTACTA) with a Tm of 60 °C.

PCR-amplified product was visualized on an agarose gel after electrophoresis and the positive samples were purified using the ExoSAP-IT PCR Product Cleanup reagent (Affymetrix, Cleveland, OH, USA).The Big Dye Terminator v3.1 Cycle Sequencing Kit (Applied Biosystems, Waltham City, MA, USA) was used for sequencing of the amplicon generated. Primers and excess dye-labeled nucleotides were first removed using the Big Dye X-terminator purification kit (Applied Biosystems). Sequencing products were run on an ABI PRISM 3130 Genetic Analyzer (Applied Biosystems).

2.7. Surface sediment sampling for cysts

Surface sediments were sampled during the dormancy period along the affected coast between February and April 2022, at water depths between 0 and 26 m using a Petite Ponar Grab or just by hand at low tide (Table 1). The upper centimeters were preserved in a labelled falcon tube and kept in the dark until further study.

About 1 gram of wet sediment was immersed in filtered seawater and, after one min of ultrasonication using an ultrasonic bath, the sediment was rinsed through a 20 μm metal mesh sieve using filtered seawater. From this residue, the cyst fraction was separated using the heavy-liquid sodium polytungstate (SPT) at a density of 1.4 g/cm (Bolch, 1997). From the total fraction, cyst concentrations were calculated using the volumetric method. Cyst concentrations were also converted into dry weight by calibrating the wet weight with dried weight.

2.8. Pigment measurements

Bloom sampling characteristics for pigment analysis are presented in Table S3. Two cultured strains were investigated: a strain previously isolated from station KE in 2003 by S. Fraga (VGO668), and the strain isolated at station CR (IFR-LI-01LC), and compared to published data from Spanish strains (LP4V and LP9V, Zapata et al., 2012). An aliquot of algal culture (5 mL) or sea water (30–50 mL) was filtered onto glass-fiber filters (GF/F 0.7 μm, 25 mm; Whatman, Maidstone, UK) and stored at

−80 °C until analysis. Filters were immersed in 2 ml of 95% acetone, sonicated for 10 min and stored at −20 °C overnight. Acetone extracts were filtered with a 0.2-μm fiberglass filter prior to injection in HPLC. The filtered acetone extracts were analyzed by HPLC-UV-DAD (series 1200 HPLC-UV-DAD; Agilent Technologies, Santa Clara, CA, USA) using an Eclipse XDB-C8 reverse phase column (150 mm × 4.6 mm, 3.5 μm particle size; Agilent Technologies) following the method described by Van Heukelem and Thomas (2001).

2.9. Toxicity of established cultures, sediments and shellfish

2.9.1. Culture extraction

The cultures of *L. polyedra* established from Le Croisic (IFR-LI-01LC) and Doëlan (IFR-CC-21–048) (CR and DO, Fig. 1) were extracted according to the protocol described below. Mixer Ball Milling equipment (Mixer Mill MM400, Retsch, Haan, Germany) was used to extract yessotoxin (YTX) and some known analogues from cells. Glass beads (150 mg, 100–250 μm in diameter) were added to the isolated cells. Samples were extracted three times by adding Methanol (Table S1) and shaking at 30 Hz for 10 min. After centrifugation at 15,000 g, the supernatants were pooled and evaporated to dryness with a gentle flow of nitrogen at a temperature of 30 °C. The residue was dissolved in 300 μl of methanol, ultrafiltered (0.20 μm, Nanosep MF, Pall, NY, USA) and transferred into a HPLC vial before LC-MS/MS analyses.

2.9.2. Sediments extraction

The sediment was sampled during the dormancy period at Pornichet (PO, Fig. 1) on the 23rd February. Four aliquots were extracted according to the protocol described below. Glass beads (2.5 g, 100–250 μm in diameter + 2.5 g, 750–1000 μm in diameter) were added to 5 g of sediment. Samples were extracted twice by adding 5 ml of Methanol and shaking at 30 Hz for 30 min (Mixer Mill MM400, Retsch). After centrifugation at 3700 g, the supernatants were pooled and evaporated to dryness with a gentle flow of nitrogen at a temperature of 30 °C. The residue was dissolved in 1000 μl of methanol, ultrafiltered (0.20 μm, Nanosep MF, Pall) and transferred into a HPLC vial before LC-MS/MS analyses.

2.9.3. LC-MS/MS analysis

Culture and sediment samples analyses were performed by LC-MS/MS using a Shimadzu UFLCxr system coupled to a triple quadruple hybrid mass spectrometer Q-Trap (API400QTrap, SCIEX, Framingham, MA) equipped with a heated electrospray ionization (ESI) source. Data acquisitions were performed using negative ion mode and MRM (Multiple Reaction Monitoring) mode. Chromatographic separation was carried out on a reversed-phase column Xbridge BEH C18 (50 × 2.1 mm, 2.5 μm, Waters) equipped with a guard column (5 × 2.1 mm, 2.5 μm, same stationary phase as column). Water (A) and acetonitrile 90% (B) both containing 6.7 mM of ammonium hydroxide were used as mobile phases at a flow rate of 400 μl.min^{-1}. The following gradient was used: 0 min, 5% B; 1.50 min, 5% B; 4.5 min, 65% B; 5.00 min, 100% B; 7.00 min, 100% B; 7.50 min, 5% B; 12.00 min, 5% B. The oven temperature was 30 °C and the injection volume was 5 μL. The LC-MS/MS methods were used to detect 22 toxins (Table S1). The ESI interface operated using the following parameters: curtain gas 20 psi, temperature: 600 °C, gas1 60 psi; gas2 60 psi, ion spray voltage −4500 V. For detection, the parameters were as follows: the declustering potential was −105 V and the entrance potential −10 V. Two collision energies (Q3_01: −46 eV; Q3_02: −42 eV) and two collision cell exit potentials (Q3_01: - 9 V; Q3_02: −11 V) were applied and the dwell time was 30 ms. The transitions that were used for the MRM mode are presented in Table S2. Quantification was performed relative to the YTX standard (National Research Council Canada, NRCC) with a 6-point calibration curve. The limit of quantification was 0.03 ng/mL for the YTX standard.

2.9.4. Toxicity of shellfish

Data were collected within the framework of the French monitoring program for phycotoxins in marine organisms (REPHYTOX, 2022). The data were obtained through the regulatory monitoring operated by the laboratory Inovalys. The REPHY guidelines (Neaud-Masson et al., 2023) define the alert threshold for *L. polyedra* as 10,000 cells/L. Weekly monitoring of phytoplankton in the water and yessotoxins in shellfish was therefore carried out as long as this threshold was exceeded. Analyses of regulated yessotoxins (YTX, homo-YTX, 45-OH-YTX, homo-45-OH-YTX) were carried out on all species of exploited shellfish (mussels, common cockles, clams, Pacific oyster), according to the official method ANSES LSA-INS-0147 (Version 4, February 2018).

Briefly, after the shellfish (1 to 2 kg) were washed with tap water, the flesh was removed from the shell and then mixed with a knife blender. Afterwards, (2.00 ± 0.05) g of this homogenate were extracted twice by adding 9 mL of methanol and homogenizing for 2 min at approximately 10,000 rpm. After centrifugation, the supernatants were transferred and pooled into a 20 mL volumetric flask completed by adding methanol. After a solid phase extraction step, the extract was filtered and transferred into a HPLC vial before LC-MS/MS analyses at the Inovalys laboratory.

2.10. Long-term records of L. polyedra

Cell counts of *L. polyedra* were extracted from the REPHY dataset since 1990 (REPHY, 2022). Observations from the citizen participation project PHENOMER were also used in this study.

3. Results

3.1. Bloom dynamics

The first significant number of cells of *L. polyedra* (15,000 cells/L) were observed in Vilaine Bay at OL during summer on the 5th of July (Fig. 2a). The onset of *L. polyedra* occurred during a bloom of diatoms, which was characterized by high numbers of specimens belonging to the *Pseudo-nitzschia delicatissima* complex on the 1st and 5th of July at BM and OL, respectively. The bloom of diatoms was then dominated by *Leptocylindrus* sp., and lasted until the end of July, with maximum numbers around the 20th of July at both BM and OL. During the bloom of diatoms, an increase in *L. polyedra* concentration was observed in the Vilaine Bay (Fig. 3). In particular, high numbers were reached at OL (28,000 cells/L) and KE (94,000 cells/L) on the 27th of July.

During early August, the microphytoplankton was dominated by dinoflagellates, with high concentrations of *L. polyedra* and/or *L. chlorophorum* (Fig. 2). In the Vilaine Bay, a brownish / reddish seawater discoloration associated with high numbers of *L. polyedra* (325,000 cells/L) and *L. chlorophorum* (500,000 cells/L) at OL was observed on the 2nd of August. High concentrations of *L. chlorophorum* were still present on the 10th of August at OL (1,000,000 cells/L). The concentration of *L. chlorophorum* then decreased rapidly from the 17th of August. In contrast, significant increases in *L. polyedra* numbers were seen near OL (2,700,000 cells/L) on the 10th of August, and in ND (2,000,000 cells/L) on the 17th of August. From mid-August, the bloom of *L. polyedra* extended beyond the Vilaine Bay, expanding first southward toward the Loire River estuary, and then north-westward at the end of the month (Fig. 3).

Numbers of *L. polyedra* remained high on several sampling points until early September, and the bloom was well visible on aerial photographs (Fig. 4), with highest concentrations on the 6th of September at ND (2,000,000 cells/L), DO (3,600,000 cells/L), and near OL (3,200,000 cells/L). After this period, the numbers declined until a last peak at Port Bélon (PB) (777,000 cells/L), CR (139,600 cells/L), and BM (150,800 cells/L) on the 14th of September. Towards the end of the bloom, *L. polyedra* may have been grazed by *Noctiluca scintillans*, which was first observed on the 17th of August and reached a peak on the 30th of
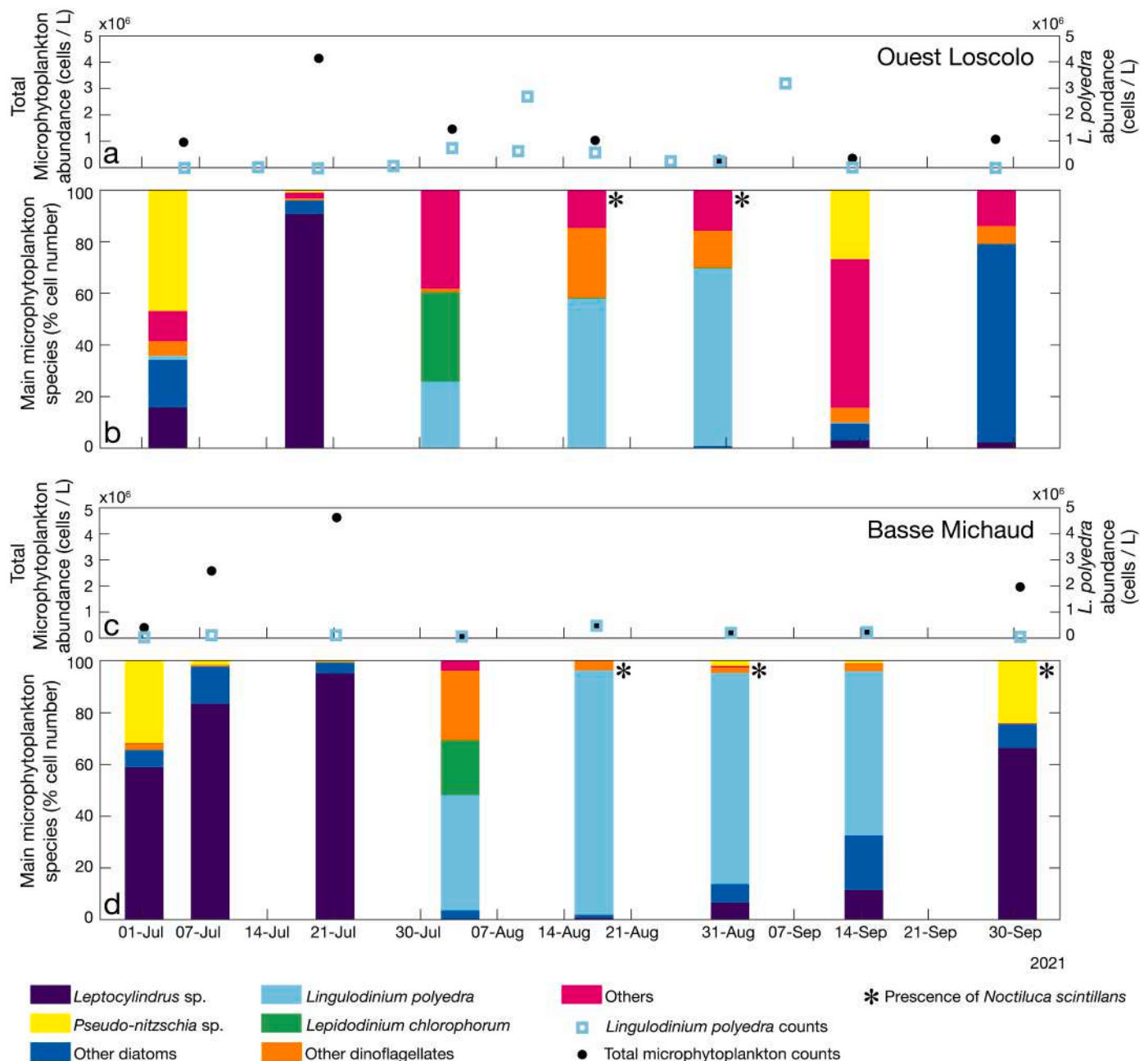
Fig. 2. *L. polyedra* cell concentrations and assemblage changes in the plankton observed at Ouest Loscolo (OL) (a, b) and Basse Michaud (BM) (c, d) throughout the summer of 2021.

September at OL (see symbol * in Fig. 2). The bloom was terminated by mid-September, and the last observation of *L. polyedra* in field samples was on the 20th of September (Fig. 3). Typical cyst formation of *L. polyedra* was observed at OL in the plankton at the end of the bloom, from mid-August to mid-September, with a maximum of 30,000 cysts/L on the 7th of September (Fig. 5).

Alexandrium tamarense occurred in the Vilaine estuary in mid-September. Maximum concentrations of this species were recorded at coastal sites, such as KE on September 13 (300,000 cells/L), where more offshore sites had much lower concentrations, such as OL which had maximum concentrations of 4100 cells/L on September 28.

3.2. Satellite images of [Chl a]

Sentinel-3/OLCI satellite observations made it possible to better appraise the spatial and temporal variability of the bloom, using the remotely-sensed [Chl *a*] as a proxy of phytoplankton biomass in the first optical layer of the water column (typically < 5 m). During the bloom of diatoms, satellite-derived [Chl *a*] increased up to ~ 30 mg/m^3 around mid-July in the Loire and Vilaine River estuaries (Fig. 6). Though cloud cover hampered satellite observations, it seemed that [Chl *a*] then progressively decreased until early August. A significant increase in [Chl *a*] was then observed on the 14th of August, with several patches of [Chl *a*] > 80 mg/m^3 stretching along the coastline from the Vilaine Bay toward the Loire River estuary (Fig. 6), and coinciding with the high numbers of *L. polyedra* observed in situ (Fig. 3). While it is not possible to determine the causative species from satellite measurement, in situ taxonomic observations at both OL and BM support the hypothesis that the patches of high [Chl *a*] were mainly caused by *L. polyedra* (Fig. 2). Towards the end of August, the bloom progressively extended offshore, with a large
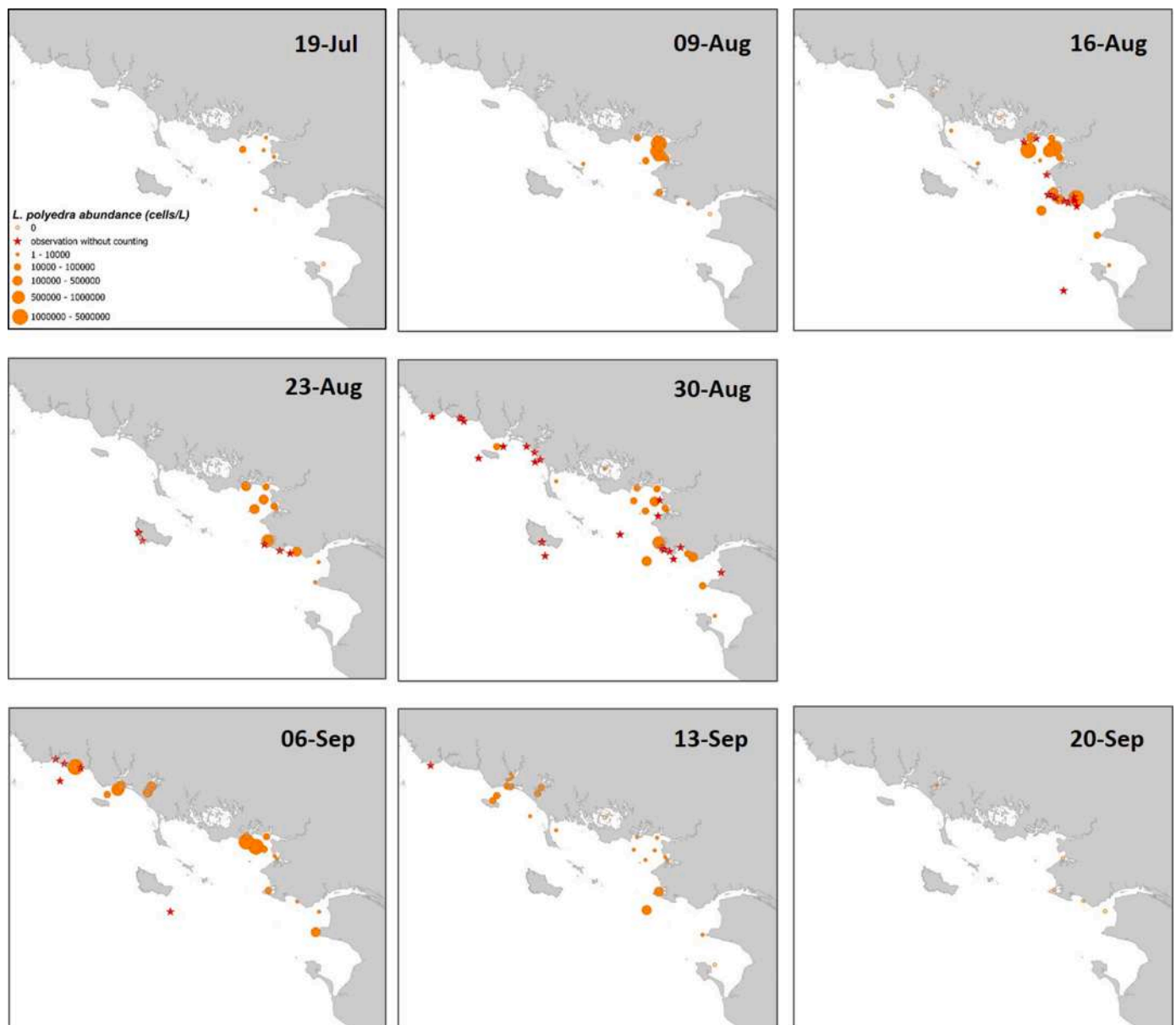
Fig. 3. Spatial and temporal changes of *L. polyedra* abundances (cells/L) observed within the framework of the REPHY network and the PHENOMER project (red stars largely denote PHENOMER observations).

patch to the southwest of Noirmoutier Island. The bloom continued to expand spatially during early September, covering a maximum extent of about 3200 km^2 on the 4th of September. From the 4th to 6th of September, highly concentrated patches of Chl *a* were observed along more than 100 km of coastline from 47°15′ to 47°45′N, as well as offshore the islands of Noirmoutier, Belle-Ile-and Groix. The [Chl *a*] within the most concentrated patches was as high as 300 mg/m^3. One of the most striking result was the sudden appearance of a large patch of about 500 km^2 with [Chl *a*] > 50 mg/m^3 south to Belle-Ile-Island within just a few days between the 31st of August and 4th of September. This large patch did not last long, and was partly dispersed two days later on the 6th of September. The bloom then progressively decreased, with [Chl *a*] dropping below 10 mg/m^3 in most parts of the study area on the 12th of September. By mid-September, the bloom had completely vanished.

3.3. Environmental parameters

The monthly river discharge by both the Loire and Vilaine rivers in July 2021 was exceptionally high compared to average July discharge, calculated between 1960 and 2020 for the Loire and between 1970 and 2020 for the Vilaine (Fig. 7). A drop in salinity recorded at the ND station (MOLIT) during the second half of July coincided with the high flows of both rivers, in particular that of the Loire (Fig. 8a). The drop in salinity was accompanied by a sharp rise in sea surface temperature (SST) and air temperature (Fig. 8b). At the ND station, the buoy MOLIT registered a maximum SST of 25.4 °C on the 19th of July (Fig. 8b), which is the highest value recorded since its first use in 2008 (Retho et al., 2022). Before this event, high [Chl *a*] was observed at ND in Vilaine Bay (~ 13 mg/m^3), and at BM offshore the Loire estuary (~ 16 mg/m^3), consistent with the high numbers of diatoms observed during this period (Fig. 8c). At that time, DIP surface concentration was < 0.1 μM. At the beginning of August, DIP and DIN surface concentrations at ND and BM were respectively below 0.1 and 0.5 μM, whereas DSi concentration was

Fig. 4. Aerial photograph of Clohars-Carnoët showing the presence of the *Lingulodinium polyedra* bloom, taken on the 7th of September 2021.
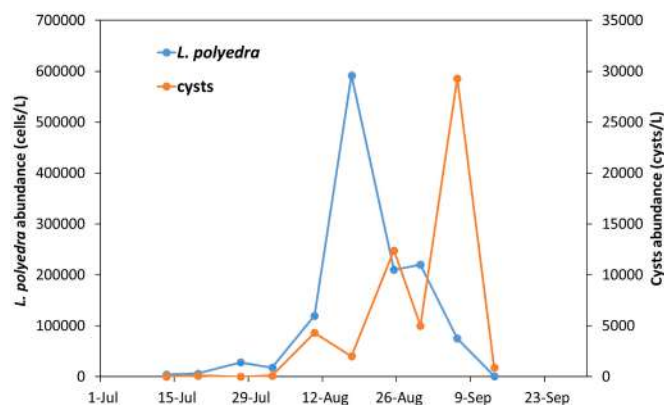

Fig. 5. Cyst abundance of *L. polyedra* (cells/L) observed in the surface water at Ouest Loscolo (OL), where water depth is 10 m.

high (Fig. 8d, e, f), suggesting a rapid consumption of the nitrogen and phosphorus nutrients brought by the river plumes. During that period, DIP and DIN concentrations in bottom waters were low, but not limiting.

In the beginning of August, colored waters of *L. polyedra* were first observed during a neap tide period (tidal range of about 4 m). During that period, the winds were weak with a speed < 10 km/h, and mainly oriented westward. In the Vilaine Bay, the water column was stratified, in terms of salinity and temperature, as shown in the recordings of the MOLIT buoy (Fig. 8b). On the 2nd August, the water temperature difference at OL was around 3 °C (surface temperature: 20.7 °C; bottom temperature: 17.6 °C, Fig. 8), and the salinity difference was around 4 (surface salinity: 33.7; bottom salinity: 29.9). The water column remained stratified in temperature throughout the bloom period. The vertical distribution of Chl *a* fluorescence at OL was quite heterogeneous, displaying either a maximum around the thermocline, or a sub-surface maximum (Fig. 9). On the 17th of August, a peak in surface [Chl *a*] corresponding to high concentrations of *L. chlorophorum* and *L. polyedra* was observed at ND (~ 35 mg/m³) and BM (~ 15 mg/m³). The increase in [Chl *a*] was accompanied by an increase in surface DIP concentration, while NID concentration remained very low, below limits of quantification. Surface DIP concentration became below 0.1 μM again

in mid-September. The average wind speed remained < 15 km/h throughout the bloom period. A change in wind direction occurred on the 23rd of August, with easterly winds coinciding with the offshore extension of the bloom (Fig. 6).

Two distinct moments of hypoxia in bottom waters could be identified at PM, concomitant with a neap tide: the first at the beginning of August and the second around the 20th of August, with a minimum dissolved oxygen concentration of 2.2 mg/L and 3.2 mg/L, respectively (Fig. 10). Very high concentrations of dissolved oxygen (up to 15 mg/L) were recorded during the bloom climax between the 4th and 6th September.

3.4. Morphological identification of cells and cysts and molecular identification of culture

Cells of *L. polyedra* displayed the characteristic shape and tabulation (*5′, 0a, 6′′, 6c, 6S, 5′′′, 2p, 1′′′′; Fig. 11; see Carbonell-Moore et al., 2021, their Table 2). A ventral pore could also be observed. The plate overlap was as described by Tillmann et al. (2021), their Fig. 6). On the 2nd August, in the sample from KE, the cell length was 33.6 (46.3) 59.6 μm (*n* = 20), the cell width was 30.8 (45.2) 62.0 μm (*n* = 20). The transparent, spherical cysts bore the typical tapering, hollow, non-tabular processes with spinules. The cyst body diameter, measured in the same sample was 44.6 (45.7) 47.6 μm (*n* = 6), and the process length was 7.9 (12.6) 19.3 μm (*n* = 18).

ITS (OQ608805, 540 bp) and LSU (OQ621602, 931 bp) sequences obtained from the cultures IFR-CC-21–048 and IFR-CC-21–049 were identical and are considered indistinguishable from the *L. polyedra* sequences MW267279 from the type locality by Tillmann et al. (2021). It is notable that there were eight ambiguous nucleotides in our LSU sequence, and four in the LSU sequence from the type locality.

3.5. Pigment analysis of cultures and environmental samples

The bloom was sampled for pigment analysis and *L. polyedra* cell number enumeration in the beginning of September (Table S3). The observed pigments, namely chlorophyll *a* and *c2* (Chl *c2*), β-carotene, diadinoxanthin, dinoxanthin, peridinin, and sometimes diatoxanthin (Fig. 12), were characteristic of dinoflagellates with type 1 chloroplasts (Gonyaulacales, Gymnodiniales, Peridiniales, Prorocentrales,
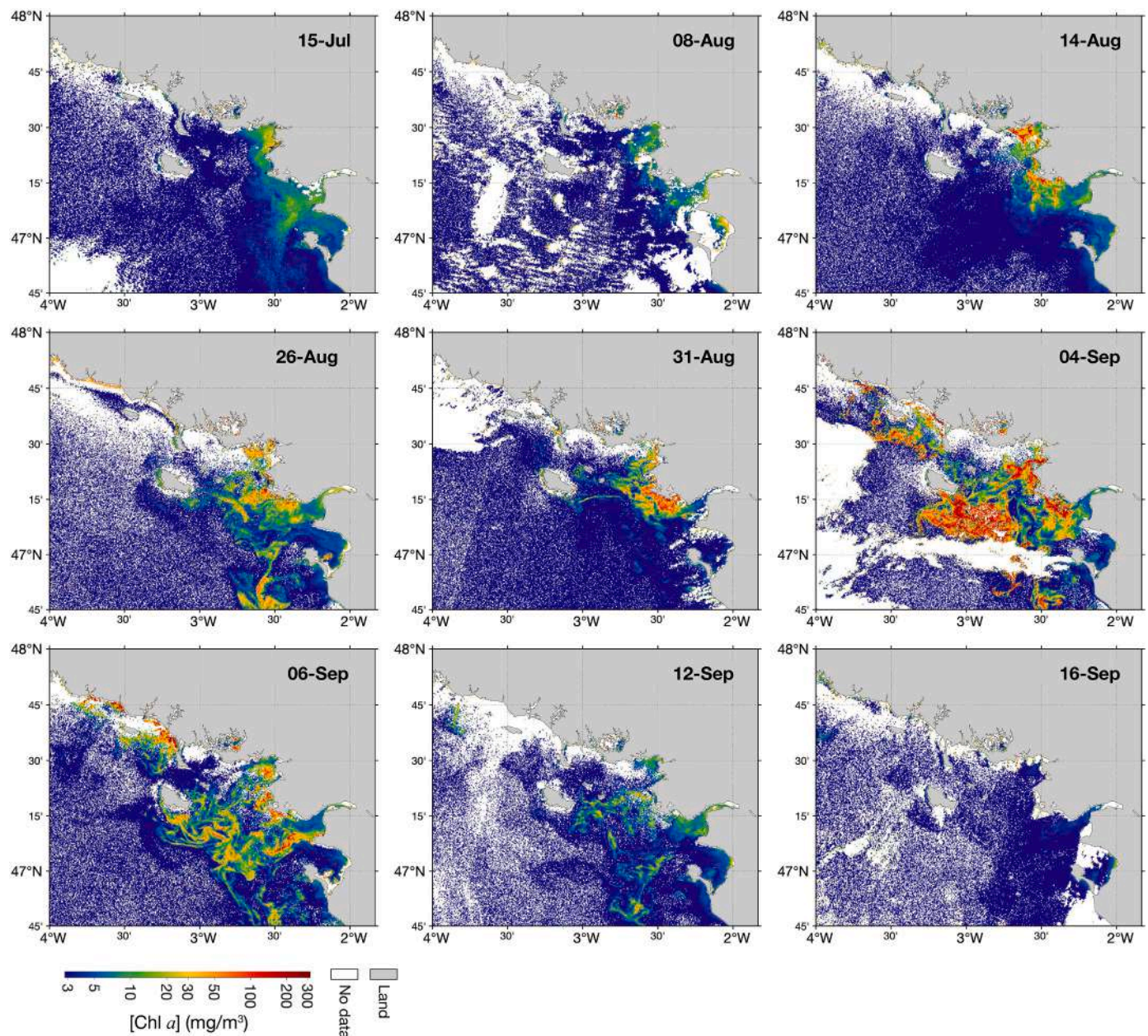
Fig. 6. Satellite images. High spatial resolution (300 m) Sentinel-3/OLCI derived maps of [Chl *a*] computed using an algorithm optimized for highly concentrated phytoplankton blooms (Smith et al., 2018). Among cloud-free satellite acquisitions, the dates were selected to (i) concisely depict the bloom development, climax, and decline, and (ii) complement in situ observations shown in Fig. 3.

Thoracosphaerales; Zapata et al., 2012), consistently with the very high number of *L. polyedra* cells. The pigment composition of the field samples was compared with those of *L. polyedra* monospecific cultures (VGO668, LP4V, LP9V, and the new strain IFR-LI-01LC) and no significant differences were found (Fig. 12). In addition, no pigments from other algal groups were detected. These results suggest that most of the observed Chl *a* belonged to *L. polyedra* or possibly other dinoflagellates with type 1 chloroplasts. Chl *a* per *L. polyedra* cell in the bloom (~36 pg/cell) was very similar to what we found in monospecific cultures (~ 41 pg/cell in the bloom strain in culture and 47 pg/cell in VGO668), and consistent with previous studies (20–60 pg/cell in Prézelin and Matlick, 1983). Nitrogen (N) content of *L. polyedra* cells in culture (~45 pmol/-cell) was also in the range of published data on *L. polyedra* (35–70 pmol/cell in Prézelin and Matlick, 1983).

3.6. Toxin concentrations of cultures, sediments and shellfish

None of the 22 yessotoxins were detected in both analysed strains IFR-CC-21–048 and IVT-LI-01LC. The detection limits were between 0.0024 and 0.024 fg/cell for these samples. Yessotoxin was however detected in sediment collected at PO in February 2022. The mean YTX concentration was 6.5 ± 0.9 ng/g dry sediment; however, none of the other yessotoxins monitored were detected. In shellfish, the highest YTX concentration was observed in mussels, with 747 µg eq. YTX/kg at Le Maresclé (LM, Fig. 1) during early September. Such level is however far below the regulatory norm of 3.75 mg eq. YTX/kg (Fig. 13). Common cockles (*Cerastoderme edule*), clams (*Ruditapes philippinarum*), Pacific oyster (*Magallana gigas*) were also contaminated, but at a level much lower than in mussels (Fig. 14).
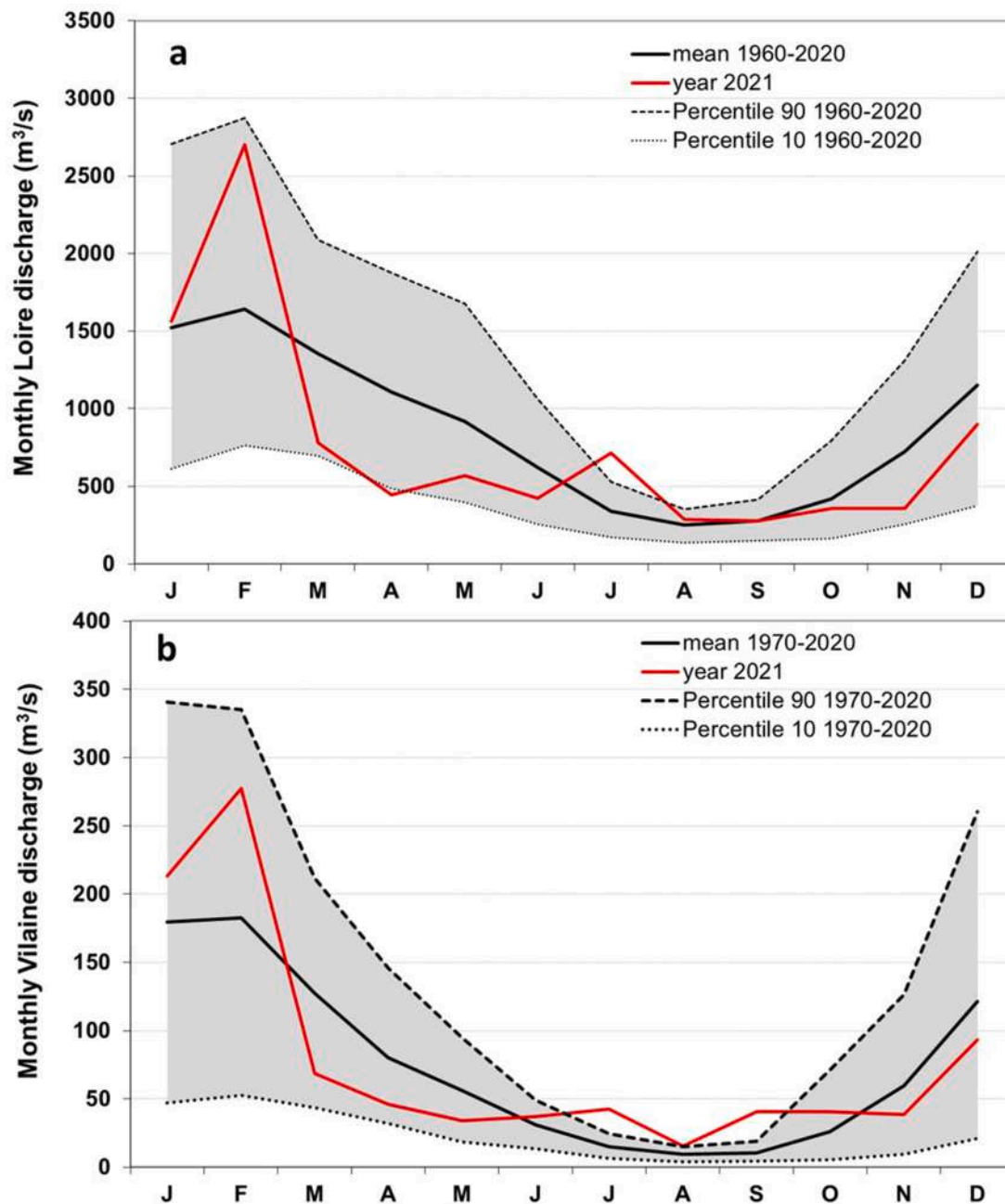
Fig. 7. Monthly river discharge (m³/s) by the Loire (a) and Vilaine (b) in 2021 compared with the mean, percentile 90 and percentile 10 from 1960 to 2020 for the Loire and 1970 to 2020 for the Vilaine.

3.7. Cyst relative abundances and concentrations in surface sediments

During the following winter, cysts of *L. polyedra* were very dominant in the assemblages with relative abundances between 67.1 and 99.3%. Other remarkable species identified were *Alexandrium minutum* (29.5% of cysts at DO), *A. tamarense* (0.06–0.75% of cysts at several locations), and *Protoceratium reticulatum* (0.06–1.5% of cysts at several locations). *Spiniferites belerius, S. lazus,* and *S. membranaceus* were also identified, but at relatively low abundances. Cysts of the autotrophic species *Biecheleria* sp., *Blixaea quinquecorne, Gymnodinium aureolum, G. impudicum, Pentapharsodinium dalei, Scrippsiella lachrymosa,* and *Sourniae diacantha* were also encountered throughout the study area. Cysts of the heterotrophic species *Archaeperidinium minutum, A. saanichi, Dissodinium pseudolunula, Dubridinium* sp., *Selenopemphix quanta, Trinovantedinium applanatum, Votadinium rhomboideum,* and *V. spinosum,* as well as round

brown cysts, spiny brown cysts, and cysts of species within the Diplopsaloideae co-occurred in the same samples. Cysts of *L. chlorophorum* were not observed in the sediment samples.

Cyst concentrations of living *L. polyedra* were quite variable, with low concentrations of 111 cysts/g dried weight at St. Gildas (SG), and highest concentrations of 94,498 cysts/g dried weight at PO (Figs. 15 and 16). There was a clear relationship between cyst concentration and sediment grain-size: fine-grained sediment had the highest concentrations. It is notable that high concentrations of the toxic species *A. minutum* were found at DO (Fig. 1) (10,680 cysts/g dried weight).

3.8. Long-term records of cell concentrations

Records of *L. polyedra* in the French Atlantic date back to August 1990, where it was identified from Prat-Ar-Coum in the North of
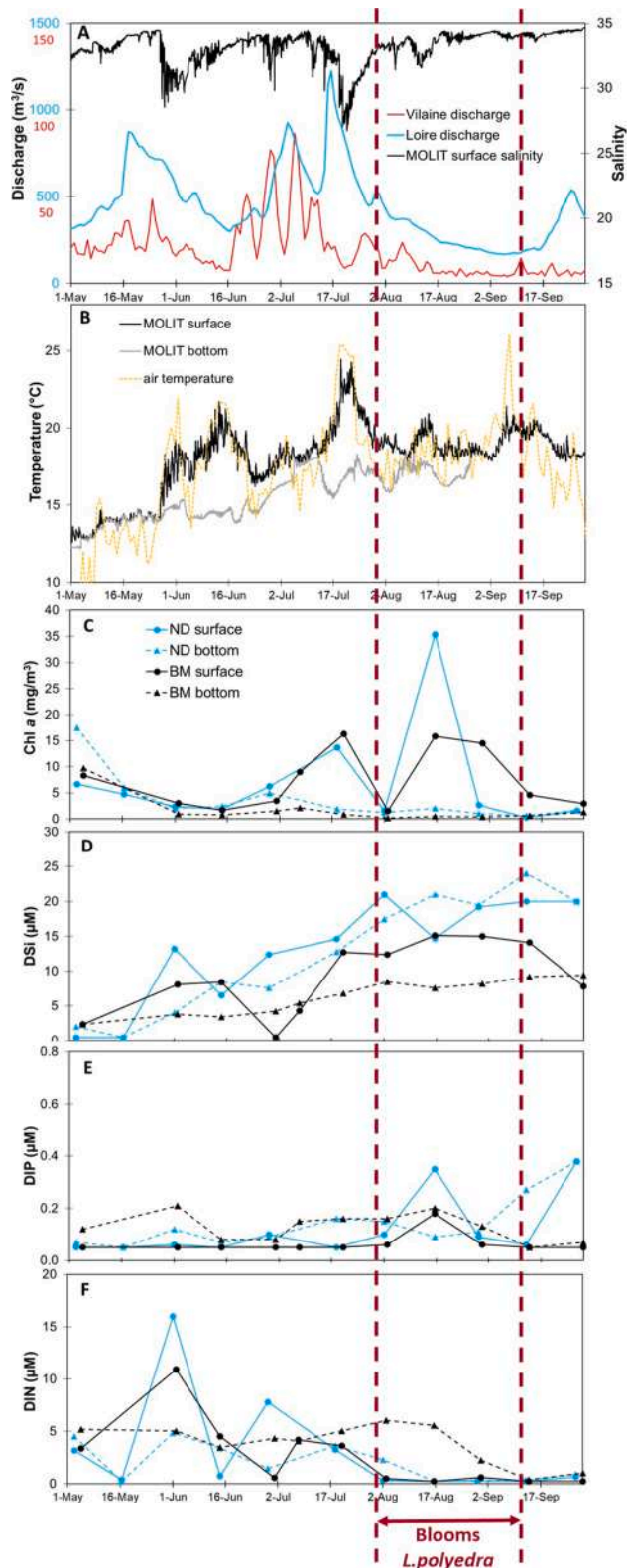
Fig. 8. Variations of environmental parameters from May to September 2021 (A) Variations in daily river discharge (m^3/s) of the Loire and the Vilaine and salinity recorded at high-frequency by the MOLIT buoy at Nord Dumet (ND) station. (B) Time-series of temperature recorded at high-frequency by the MOLIT buoy at ND station, and air temperature at the weather station Vannes-Séné. (C) Chl a (µg/L) in surface water at ND. (D–F). DSi, DIP and DIN concentrations (µM) at ND and BM stations. Vertical dashed lines indicate period when blooms were observed in situ.

Brittany (REPHY, 2022). Since then, *L. polyedra* has occurred in low concentrations, with the exception of two events in August 2003 at Le Halguen in southern Brittany (38,000 cells/L) and September 2017 at Hossegor in the Landes (187,000 cells/L) (REPHY, 2022) (Fig. 17). This suggests that the bloom reported in this study was unprecedented.

4. Discussion

4.1. Identification of L. polyedra

The typical shape and tabulation described by Tillmann et al. (2021) identifies the species morphologically as *L. polyedra*, and the measurements also conform to observations provided by these authors: 37.6–52.5 µm in length and 33.8–47.9 µm in width. The LSU and ITS rDNA sequences confirm this identification. The observed cysts also conform to the description given by Van Nieuwenhove et al. (2020), and their sizes fit the wide ranges reported by the same authors (35–60 µm in body diameter and 0–35 µm in process length).

4.2. From cells to satellite: importance of observation strategy

The synergetic use of taxonomically-accurate point-based field monitoring together with opportunistic citizen seawater discoloration reports and spatially-resolved [Chl a] satellite time-series made it possible to provide an accurate picture of the bloom dynamics in terms of phytoplankton composition, concentration, and spatiotemporal variability. While regular, station-based monitoring such as the REPHY program was instrumental to characterize phytoplankton abundance and diversity (Fig. 2), the citizen science project PHENOMER has significantly aided in documenting the bloom. Seven reports of colored water during summer 2021 have enabled to better document the bloom extent and duration (Fig. 3, red stars largely denote PHENOMER observations). This highlights the importance of citizen participation in complement of regular monitoring to study HABs in nearshore waters. In addition, Sentinel-3/OLCI observations made it possible to provide consistent pictures of the bloom up to 100 km off shore, in otherwise under-sampled areas. Due to the considerable size of the bloom, the spatial resolution (300 m) and wide swath of S3/OLCI were appropriate for accurate mapping over a large region (i.e. > 10,000 km^2). Whereas blooms of *L. polyedra* generally extend over large scales (e.g. Pitcher et al., 2019, Kahru et al., 2021), seawater discolorations caused by other dinoflagellates may be much smaller, with spatial features < 300 m. In that case, satellite sensors with a higher spatial resolution such as Sentinel-2/MSI (20 m) would be more performant than S3/OLCI, as recently demonstrated for a variety of red tide events worldwide (Gernez et al., 2023), including high-biomass blooms of *L. chlorophorum* (Roux et al., 2022) and *N. scintillans* (Sacilotto Detoni et al., 2023). On the other hand, due to its high temporal resolution, S3/OLCI (1 day) is more suited than S2/MSI (5 days) for short-term temporal studies. In the present study, the high temporal resolution of S3/OLCI made it possible to acquire enough cloud-free images to document the bloom dynamic during a gloomy summer.

4.3. Unprecedented concentrations and relation to toxicity and oxygen concentrations

Extremely high concentrations of *L. polyedra*, in the range from 2,000,000 to 3,600,000 cells/L, were observed in situ at several stations from mid-August to early September. The combined interpretation of both the satellite-derived Chl a concentration (up to 300 mg/m^3 in the most intense patches during early September) together with the in situ measurement of *L. polyedra* intra-cellular Chl a content (36 pg Chl a/cell) suggests that *L. polyedra* maximal cell number was of the order of 8,000,000 cells/L during the bloom climax. The occurrence of such high concentrations of *L. polyedra* and the sheer size of the bloom for the first time in over thirty years, is quite impressive, and highlights that a
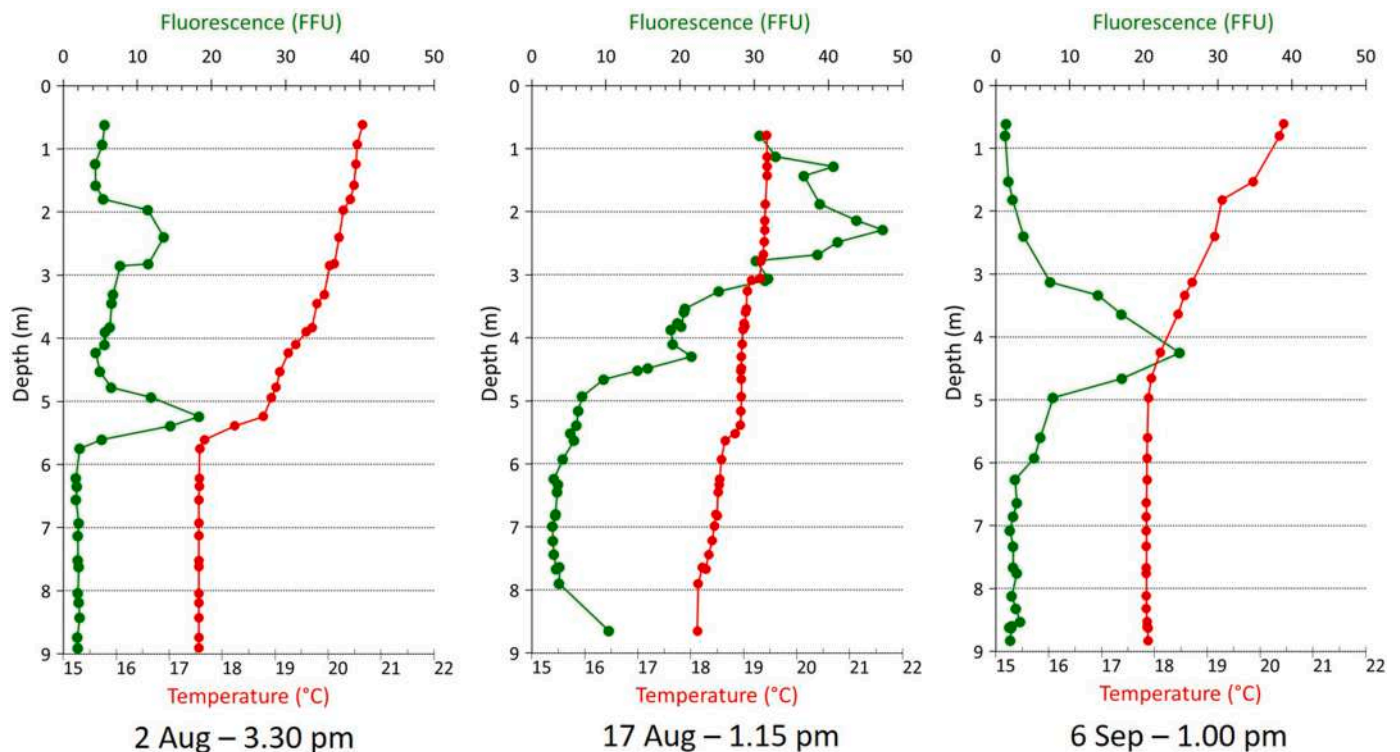
Fig. 9. Fluorescence and Temperature profiles at Ouest Loscolo (OL) on August 2nd, August 17th and September 6th 2021.
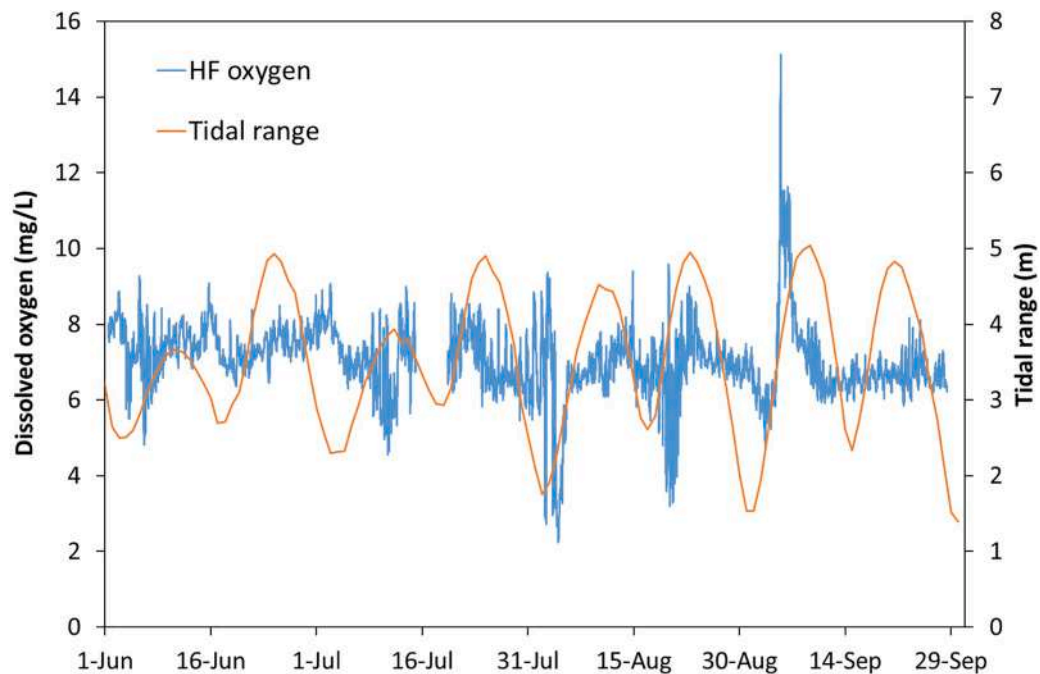

Fig. 10. Oxygen concentrations (mg/L) in bottom waters at Pont Mahé (PM), and tidal coefficients from June to September 2021.

tipping point, an abrupt shift in ecosystem state, was reached because a massive change in the environment has occurred. However, these are not the highest concentrations that have been reached worldwide: highest concentrations ever were one order of magnitude higher: 56,100,000 cells/L as recorded from Odessa Bay by Terenko and Krakhmalny (2021) and similar high numbers have been recorded from Kaštela Bay (e.g., 44,000,000 cells/L; Marasović et al., 1995), California (e.g. 27,700,000 cells/L; Eppley and Harrison, 1975), and Mexico (15,

414,000 cells/L; Stohler, 1959).

Although no toxicity was detected for the established cultures, toxins were detected in the cyst-containing sediments, and in several shellfish species that were contaminated during and after the bloom, suggesting that *L. polyedra* produces YTXs, but at low concentrations. The cultured *L. polyedra* strains could have lost their toxicity, could have never been toxic, or could produce toxins below detection levels. The other YTX producers, *Protoceratium reticulatum* and *Gonyaulax spinifera*, were
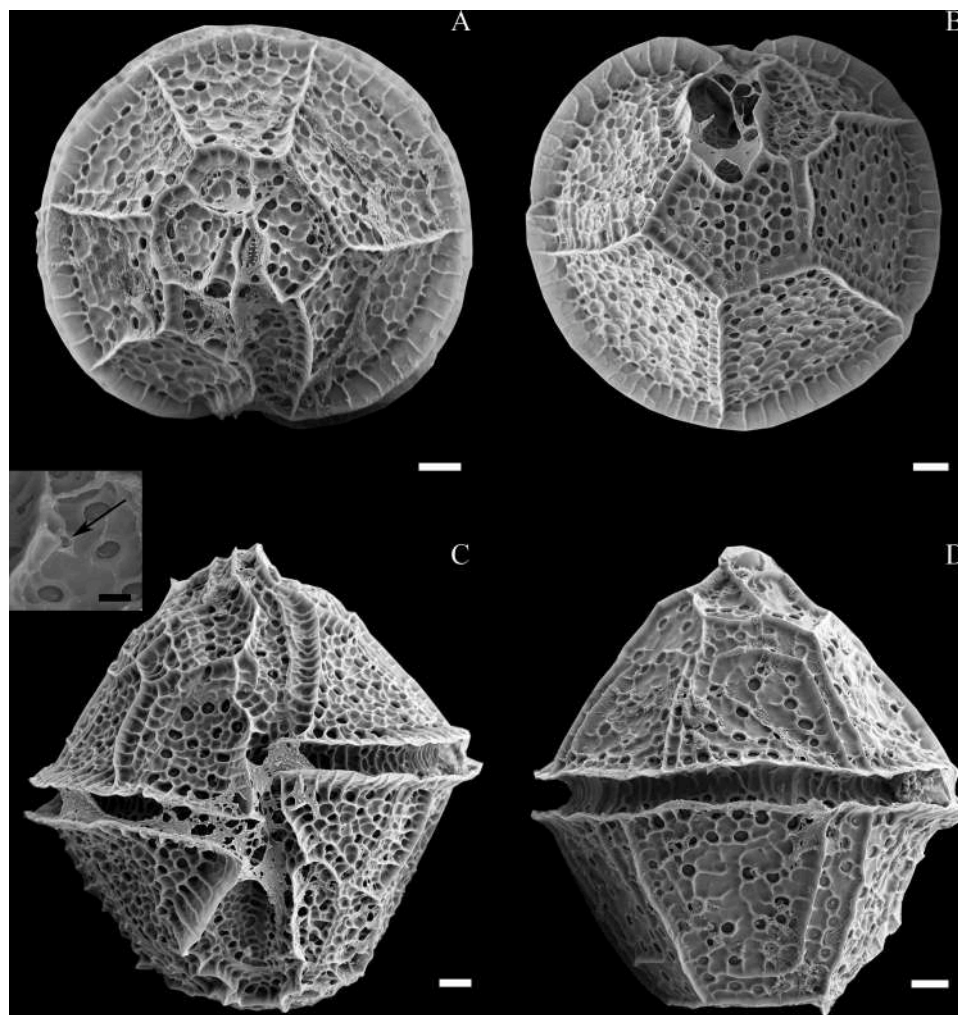
Fig. 11. Scanning electron micrographs of *L. polyedra* from Kervoyal (KE). (A) Apical view. (B) Antapical view. (C) Ventral view and detail of other cell showing presence of ventral pore (denoted by black arrow). (D) Dorsal view. All scale bars = 3 μm.
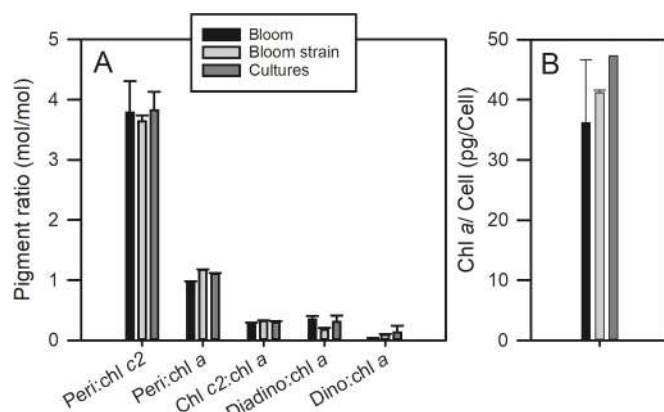

Fig. 12. Pigment composition of *Lingulodinium polyedra* in the bloom and in monoalgal cultures. (A) Pigment ratios (mol/mol): Peridinin/Chl c2, Peridinin/Chl *a*, Chl *c2*/Chl *a*, Diadinoxanthin/Chl *a*, Dinoxanthin/Chl *a*. (B) Chl *a* per cell (pg/cell). Each bar is the mean of 12 different samples for the bloom data, the mean of three different strains (LP4V, LP9V from Zapata et al. (2012) and VGO668) for the culture data and the mean of four cultures for the strain IFR-LI-01LC. Error bars represent standard deviations.

rarely present or absent in the plankton and sediment samples, and can thus not explain the presence of YTXs. Toxic episodes that have previously been associated with blooms of *L. polyedra* displayed elevated YTXs concentration in mussels (North Adriatic Sea: Tubaro et al., 1998; NW Spain: Arévalo et al., 2006; Black Sea: Morton et al., 2007).

Mortalities have also been associated with such blooms: mortality of abalone in South Africa (Pitcher et al., 2019; although *Gonyaulax membranacea* was co-occurring in the bloom), oyster mortalities during summer 1964 in the Auray Estuary, France (Paulmier, 1972), mussel mortality the fall of 1962 in Alamitos Bay Marina, California (Reish, 1963) and fish and shellfish mortalities in California in 2020 (Anderson and Hepner-Medina, 2020). These mortalities could be related to the toxicity of *L. polyedra*, but have also been related to dissolved oxygen depletion (Reish, 1963; Anderson and Hepner-Medina, 2020). In our study, low oxygen concentrations were recorded in bottom waters by the high frequency monitoring at the PM station. Some concentrations were below 2.9 mg/L, the hypoxic threshold for many benthic invertebrates (Rosenberg et al., 1991; Diaz and Rosenberg, 2008) but no anoxic levels were reached and no mortalities have been observed during the study period. More severe hypoxias might have occurred in deeper and more stratified areas.

Although mentioned by Belin et al. (2021) in their review of toxic species along French coasts, *L. polyedra* was not discussed in depth, presumably because of the little variation seen in the spatial, temporal, and abundance trends. The current study documents the accumulation
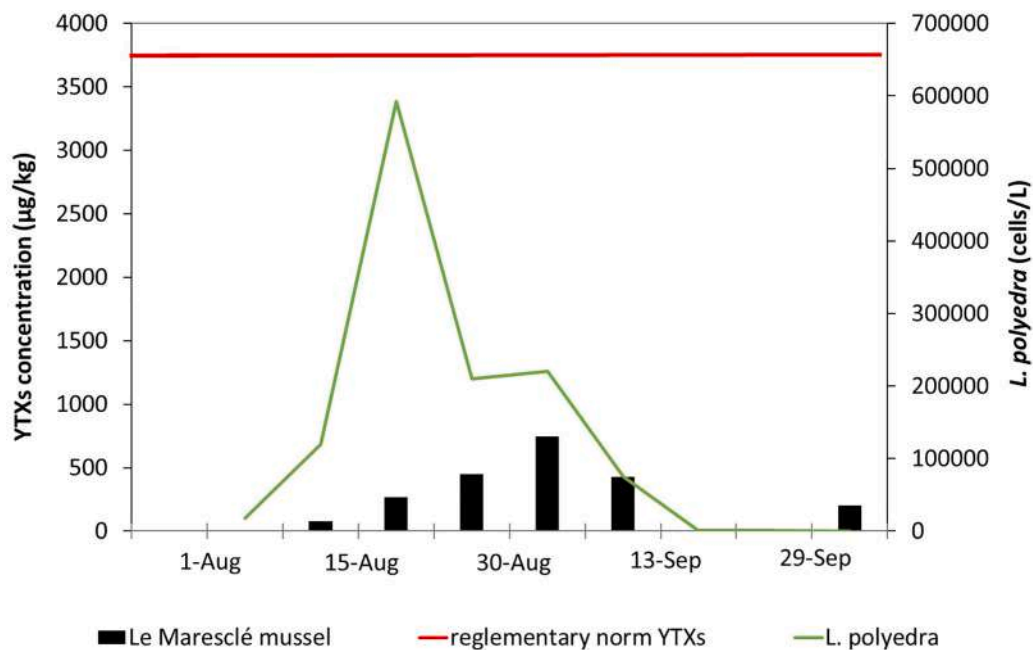
Fig. 13. YTX concentrations measured in mussels in Vilaine Bay (Le Maresclé station, LM) and *L. polyedra* concentrations (cells/L) from Ouest Loscolo (OL). Reglementary norm is indicated.
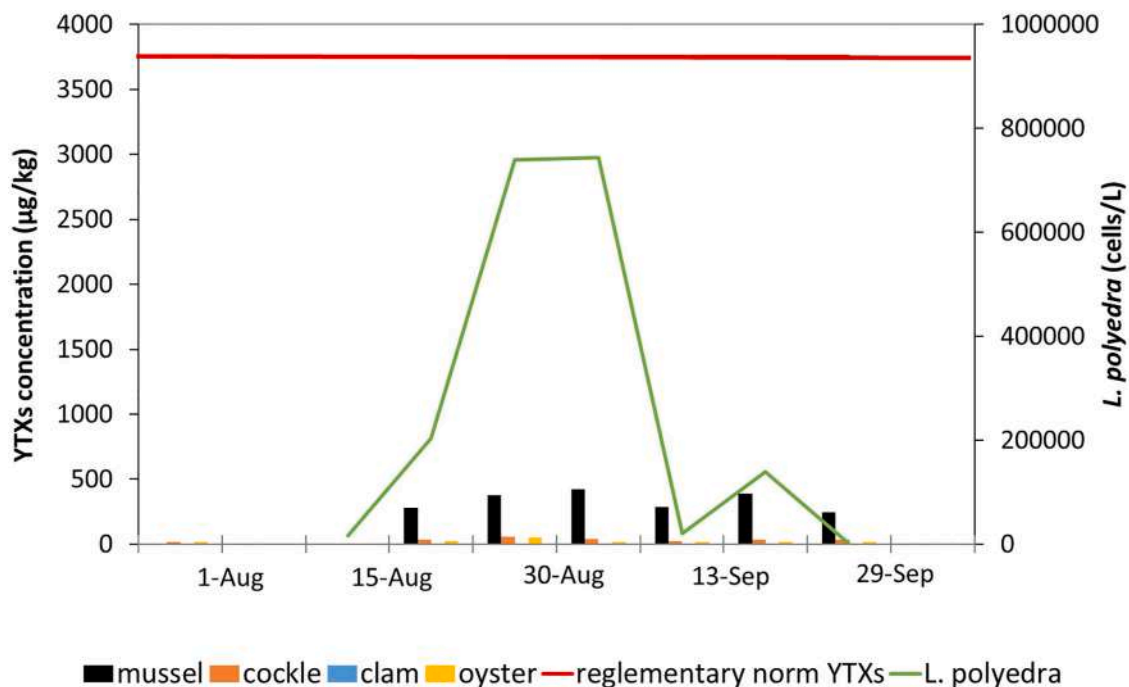

Fig. 14. YTX concentrations (µg/kg) measured in mussels and other shellfish and *L. polyedra* concentrations (cells/L) at Le Croisic (CR). Reglementary norm is indicated.

of YTXs in shellfish and hypoxia events caused by *L. polyedra* on the French Atlantic coast.

4.4. What triggered and maintained the bloom?

It is difficult to understand how all of a sudden such high concentrations were reached. There are two possible explanations as to its origin, which could be autochtonous or allochtonous. Cells or cysts could have been advected from elsewhere. However, there is no evidence of significant blooms of *L. polyedra* further to the south of France

(REPHY data) or the North of Spain during this period (Martha Revilla, pers. comm.), which makes it unlikely that the bloom was advected. In addition, 15 surface sediment samples previously screened for cysts in Vilaine Bay during winter 2018/2019, showed low abundances of *L. polyedra* cysts in the area (André, 2019; Schapira et al., 2021; Roux et al., 2023). It seems thus likely that the right environmental conditions were in place for bloom development from a small local seed population. *L. polyedra* cysts that have been stored under anoxic conditions germinate faster than those stored in an oxic environment (Blanco, 1990). Ratmaya et al. (2022) showed that the concentration of dissolved
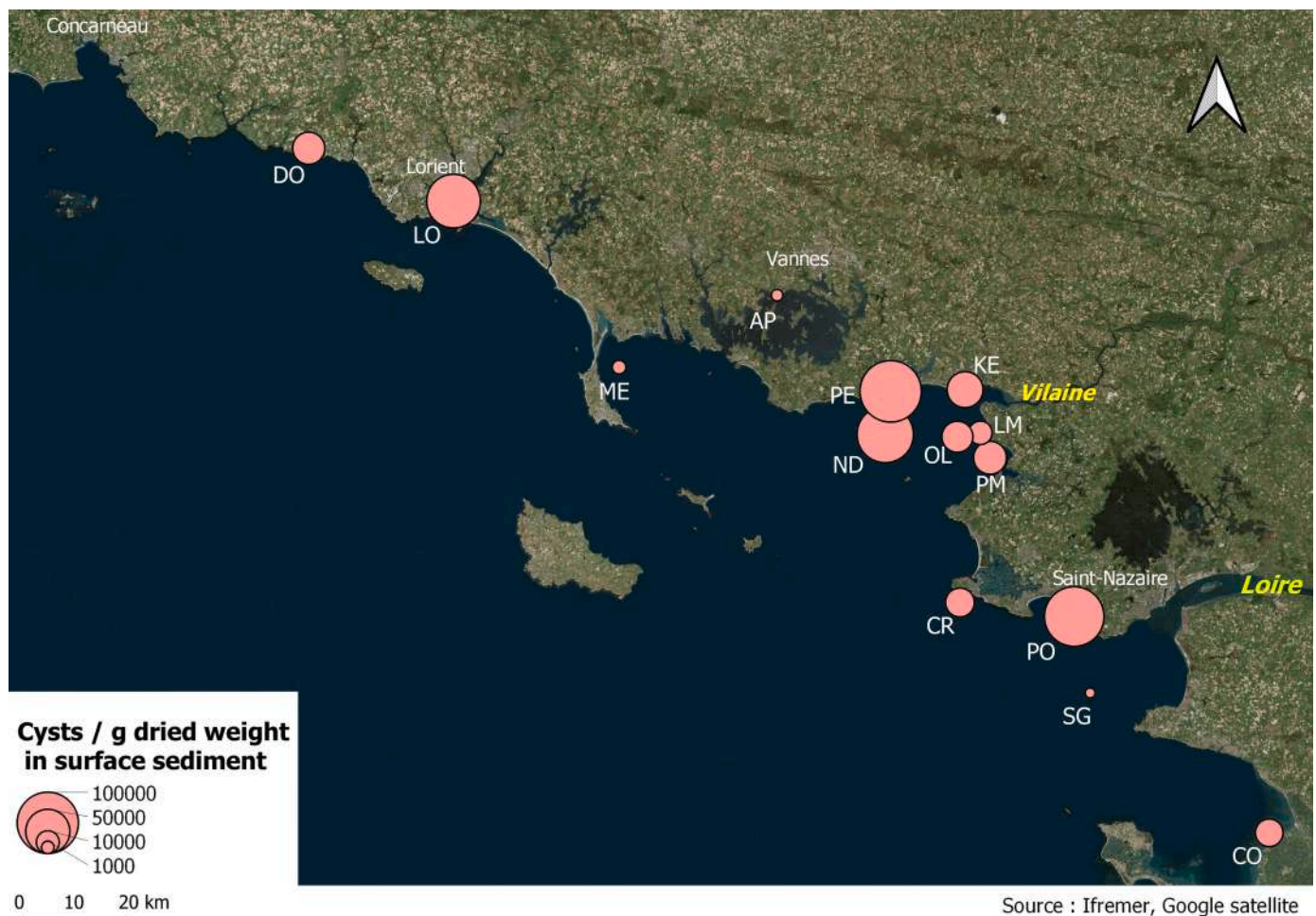
Fig. 15. Cyst concentrations in surface sediments (cysts/g dried weight) at the end of winter 2021/2022. AP = Anse de Pen Men, CO = Coupelasse, CR = Le Croisic, DO = Doëlan, KE = Kervoyal, LM = Le Maresclé, LO = Lorient harbor, ME = Men er Roué, ND = Nord Dumet, PE = Pénerf, OL = Ouest Loscolo, PM = Pont Mahé, PO = Pornichet Port, SG = Saint Gildas.

oxygen in the sediments of Vilaine Bay decreased rapidly in the first 2 mm and then was undetectable below this depth. The thickness of the oxidized layer varies according to the temperature and the intensity of the mineralization of the organic matter (Souchu et al., 2018). The sediments of Vilaine Bay therefore have favorable characteristics for the rapid germination of *L. polyedra* cysts. The bay of Vilaine, whose hydro-morphological characteristics are favorable to the development of phytoplankton, could therefore be the site of initiation of the *L. polyedra* blooms observed in southern Brittany in 2021. It is also possible that dredging activities during summer have liberated dormant cysts from the sediments (e.g. Fernandes et al., 2023), but we have no data that could support such a claim.

The unusually high river discharge and subsequent water column stratification have likely contributed to the massive development of *L. polyedra*, although measured nutrient concentrations were not unusual (cf. Ratmaya et al., 2019). High Chl *a* concentrations have indeed previously been correlated to higher river discharge in the northern Bay of Biscay (Gohin et al., 2019). The freshwater input occurred during a period of nutrient depletion, and coincided with a bloom of diatoms (*Leptocylindrus* spp.). In the Vilaine Bay, blooms of diatoms are predominantly driven by nutrient inputs associated with freshwater plumes from the Loire and Vilaine rivers (Ratmaya et al., 2022). The deposited diatom-derived OM is then mostly directly mineralized and recycled within the water column as ammonium (NH_4^+) and organic nitrogen (Ratmaya et al., 2022). These sources of nitrogen may have benefited to *L. polyedra* (see below). Moreover, in the Vilaine Bay, sediments

represent a substantial DIP source in summer (Ratmaya et al., 2019), and the increase in DIP concentrations observed in seawater around mid-August 2021 could have a benthic origin. Benthic flows of nutrients were all the more important for the development of *L. chlorophorum* and *L. polyedra* that the water mass was stratified during periods of weak winds and/or neap tide. Water column stratification is considered an essential physical condition for the proliferation of dinoflagellates (Margalef, 1978; Smayda, 2002) and it certainly contributed to the development of *L. polyedra* blooms, as suggested by Ruiz-de la Torre et al. (2013)). The fluorescence maximum was sometimes recorded at the thermocline, suggesting higher *L. polyedra* abundance at this depth. This species could migrate vertically throughout the water column to use nutrients located below the pycnocline as demonstrated or suggested for other dinoflagellates (Glibert et al., 2016; Roux et al., 2022).

DIN was limiting in surface waters from the beginning of August to the end of September according to the criteria of Fisher et al. (1995), but urea uptake very likely contributed to sustain the growth *L. polyedra*. Kudela and Cochlan (2000) demonstrated that 38% of the nitrogen demand for a *L. polyedra* red tide event in Southern California was supported by urea. *L. polyedra* is also a mixotrophic dinoflagellate (combining phototrophy and phagotrophy), able to ingest a variety of organisms, ranging from picoplankton-sized prey (< 2 μm) up to larger preys (> 30 μm, Jeong et al., 2005). Mixotrophy is important in nutrient acquisition, growth of harmful algal species, and bloom maintenance in eutrophic habitats (Burkholder et al., 2008). The important growth and persistence of the *L. polyedra* bloom over several weeks is therefore
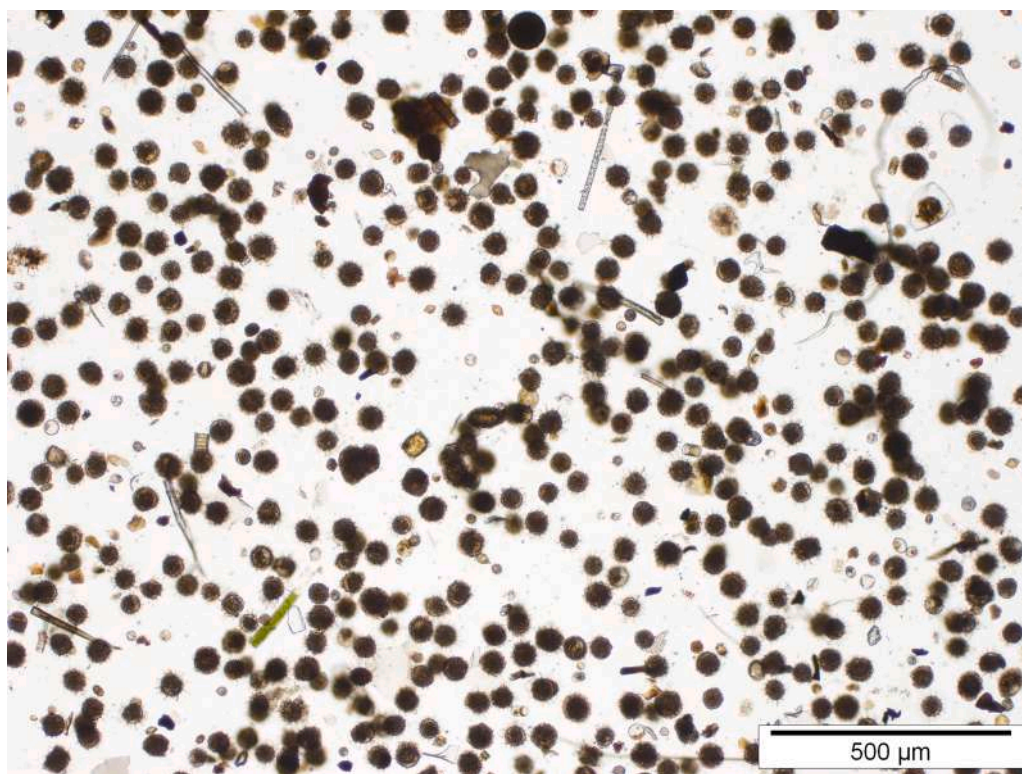
Fig. 16. Light microscope image of cysts from surface sediment from Pornichet Port (PO, 23 February 2022). Scale bar = 500 μm.

likely due to a combination of both ecophysiological (e.g., mixotrophy) and hydro-meteorological (freshwater inputs followed by a period of low wind and water mass stratification) factors. The wind played a further role as the change to easterly winds may have contributed to

disperse the bloom westwards after mid-August.

When such conditions occurred during previous summers in Vilaine Bay, it led to seawater discolorations associated with blooms of *L. chlorophorum* (Siano et al., 2020), such as in 2019 (Roux et al., 2022).
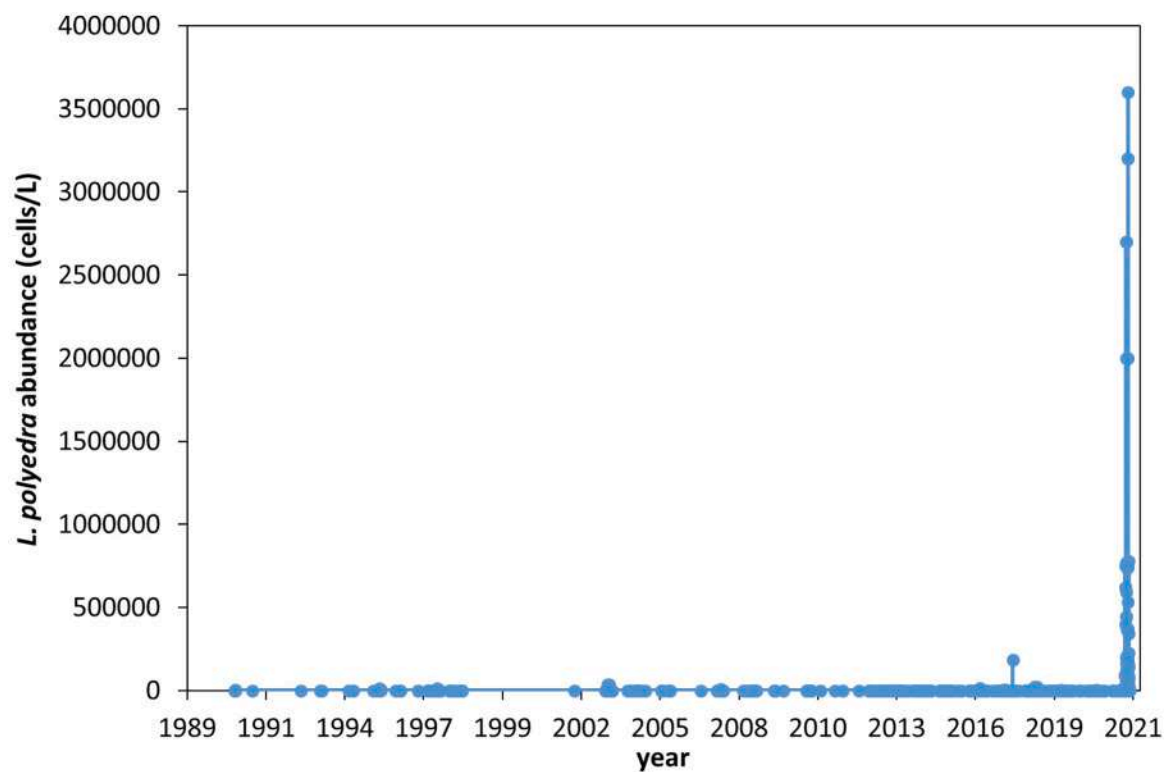

Fig. 17. Long-term record of *L. polyedra* concentrations (cells/L) recorded along the French Atlantic and Manche since 1990, extracted from the REPHY dataset (REPHY, 2022).

In 2019, the spatial extent of the *L. chlorophorum* bloom was however far smaller than the massive bloom of *L. polyedra* documented in the present study. While the exceptional rainfall that occurred in June – July certainly played a role in promoting phytoplankton growth, the reason why *L. polyedra* dominated over other HAB-forming dinoflagellate species remains to be fully elucidated .

4.5. What terminated the bloom?

Several factors have been documented in the literature to explain bloom termination in dinoflagellates, such as grazing (e.g., Busch et al., 2019), cyst formation (e.g., Wang et al., 2007; Brosnahan et al., 2017), parasite infection (e.g., Velo-Suárez et al., 2013), algicidal bacteria (Doucette et al., 1999), and/or changes in hydrodynamics (e.g., Ralston et al., 2015). Grazing and cyst formation have been observed during this study and are discussed below.

Noctiluca scintillans is a heterotrophic dinoflagellate that has been described as an effective grazer of large *L. polyedra* blooms in the Southern California Bight (Balch and Haxo, 1984; Howard, 1996; Goldstein, 2011). It could play an important role for *L. polyedra* bloom regulation and possibly even termination, as it occurs several weeks after blooms of *L. polyedra* (Busch et al., 2019). In our study area, *N. scintillans* was observed at OL and BM stations around mid-August (Fig. 2b, d). Other grazers that have been related to *L. polyedra* blooms in California are *Polykrikos* sp., *Fragilidinium heterolobum*, as well as rotifers and ciliates (Eppley and Harrisson, 1975), but such taxa have not been observed in notable numbers in the present study. Zooplankton grazers such as copepods likely do not have such an effect: *L. polyedra* has a competitive advantage because of its bioluminescence that can deter copepods (Prevett et al., 2019). It is also notable that a bloom of (presumably nontoxic) *A. tamarense* occurred in the Vilaine estuary in mid-September, right after the *L. polyedra* bloom.

Cyst production was also observed during this study in the plankton at the end of the bloom. The induction of sexuality has been presumed to be related to nutrient depletion, changes in day length, temperature, light intensity and dissolved gasses (Pfiester and Anderson, 1987, p. 631), but this was not seen in this study.

4.6. Seed banks

The very high concentrations of *L. polyedra* cysts frequently found in surface sediments demonstrate that a significant seed bank has been formed after the bloom. Concentrations of living *L. polyedra* cysts (between 111 and 100,710 cysts/g dried weight) are greater than concentrations of living cysts recorded by Lewis (1988) from Loch Creran (west coast of Scotland) (between 0 and 20,253 cysts/g dried weight), where *L. polyedra* blooms have been recurrent over many years. They are also much higher than *L. polyedra* cyst concentrations recorded in palynologically treated surface sediments from the Bay of Brest, which ranged between 49 and 3000 cysts/g dried weight (Lambert et al., 2022). However, the results from the methods used here are not directly comparable to palynological methods; both methods can introduce a numerical bias and palynological methods enumerate cysts with cell contents and those without (Mertens et al., 2009b). High concentrations of *L. polyedra* cysts related to fine grain-size conform to previous observations by Lewis (1988). The presence of such seed banks suggests that blooms of *L. polyedra* will be recurrent in the coming years. It also demonstrates that *L. polyedra* blooms are clearly imprinted in the geological record by an exponential increase in cyst numbers. This result supports the hypothesis of Dale (2009) that *L. polyedra* cysts are useful indicators of increased nutrient supplies.

The discovery of cysts of the potentially toxic species *A. minutum* at relatively high concentration at DO not only shows that *L. polyedra* had formed a seed bank, it also highlights that very local seed banks can be formed and pose a risk for local stakeholders (e.g. shellfish farms).

The presence of such important seed banks has its implications for

regional dredging or trawling activities. Such activities cause resuspension of cysts from sediments, and can provide an inoculum for blooms (e.g., Brown et al., 2013), and therefore are recommended to take place during winter.

Supplementary materials

Supplementary material associated with this article can be found, in the online version, at doi:10.1016/j.hal.2023.102426.

References

Aminot, A., Kérouel, R., 2004. Hydrologie des Écosystèmes Marins: Paramètres et Analyses. Ifremer, France, p. 336. ISBN 2-84433-133-5. [In French].

Aminot, A., Kérouel, R., 2007. Dosage Automatique Des Nutriments Dans Les Eaux marines: Méthodes En Flux Continu. Ifremer, Plouzané, France, p. 188 [In French].

Amorim, A., Palma, A.S., Sampayo, M.A., Moita, M.T., 2000. On a *Lingulodinium polyedrum* bloom in Setúbal Bay, Portugal. In: Hallegraeff, G.M., Blackburn, S.I., Bolch, C.J., Lewis, R.J. (Eds.), Proceedings of the Ninth International Conference on Harmful Algal Blooms. UNESCO Publishing, Paris, pp. 133–136.

An, K.H., Lassus, P., Maggi, P., Bardouil, M., Truquet, P., 1992. Dinoflagellate cyst changes and winter environmental conditions in Vilaine Bay, Southern Brittany (France). Bot. Mar. 35, 61–67.

Anderson, C., Hepner-Medina, M., 2020. Red Tide Bulletin. spring 2020. https://sccoos.org/california-hab-bulletin/red-tide/.

André, C., 2019. Stage De Recherches Des Kystes De L'espèce Nuisible *Lepidodinium chlorophorum* Par Approches Multidisciplinaires Au Large De La Loire et De La Vilaine. Université Sciences et Techniques de Nantes, Master 2 Sciences de la Terre et des Planètes, Environnement, parcours Ecosystèmes et Bioproduction Marine. Unpublished MSc thesis [In French].

Arévalo, F., Pazos, Y., Correa, J., Salgado, C., Moroño, A., Pan, B., Franco, J., 2006. First report of yessotoxins in mussels of the Galician Rias during a bloom of *Lingulodinium polyedrum* Stein (Dodge). In: Henshilwood, K., Deegan, B., McMahon, T., Cusak, C., Keaveney, S., Silke, J.O., Cinneide, M., Lyons, D., Hess, P.. In: Proceedings of the 5th International Conference on Molluscan Shellfish Safety, Galway, Ireland, pp. 184–189.

Armstrong, M., Kudela, R., 2006. Evaluation of California isolates of *Lingulodinium polyedrum* for the production of yessotoxin. Afr. J. Mar. Sci. 25, 399–401.

Balch, W.M., Haxo, F.T., 1984. Spectral properties of *Noctiluca miliaris* Suriray, a heterotrophic dinoflagellate. J. Plankton Res. 6, 515–525.

Belin, C., Soudant, D., Amzil, Z., 2021. Three decades of data on phytoplankton and phycotoxins on the French coast: lessons from REPHY and REPHYTOX. Harmful Algae 102, 101733.

Bennouna, A., Berland, B., El Attar, J., Assobhei, O., 2002. Eau colorée à *Lingulodinium polyedrum* (Stein) Dodge, dans une zone aquacole du littoral du Doukkala (Atlantique marocain). Oceanolog. Acta 25, 159–170 [In French with English Abstract].

Blanco, J., 1990. Cyst germination of two dinoflagellate species from Galicia (NW Spain). Sci. Mar. 54, 287–291.

Bolch, C.J.S., 1997. The use of polytungstate for the separation and concentration of living dinoflagellate cysts from marine sediments. Phycologia 37, 472–478.

Brosnahan, M.L., Ralston, D.K., Fischer, A.D., Solow, A.R., Anderson, D.M., 2017. Bloom termination of the toxic dinoflagellate *Alexandrium catenella*: vertical migration behavior, sediment infiltration, and benthic cyst yield. Limnol. Oceanogr. 62, 2829–2849.

Brown, L., Bresnan, E., Summerbell, K., O'Neill, F.G., 2013. The influence of demersal trawl fishing gears on the resuspension of dinoflagellate cysts. Mar. Pollut. Bull. 66, 17–24.

Burkholder, J.M., Glibert, P.M., Skelton, H.M., 2008. Mixotrophy, a major mode of nutrition for harmful algal species in eutrophic waters. Harmful Algae 8, 77–93.

Busch, M., Caron, D., Moorthi, S., 2019. Growth and grazing control of the dinoflagellate *Lingulodinium polyedrum* in a natural plankton community. Mar. Ecol. Prog. Ser. 611, 45–58.

Caballero, I., Fernández, R., Escalante, O.M., Mamán, L., Navarro, G., 2020. New capabilities of Sentinel-2A/B satellites combined with in situ data for monitoring small harmful algal blooms in complex coastal waters. Sci. Rep. 10, 8743.

Carbonell-Moore, M.C., Matsuoka, K., Mertens, K.N, 2021. Gonyaulacalean tabulation revisited using plate homology and plate overlap, with emphasis on the ventral area (Dinophyceae). Phycologia 61, 195–210.

Chapelle, A., Lazure, P., Ménesguen, A., 1994. Modelling eutrophication events in a coastal ecosystem. Sensitivity analysis. Estuar Coast Shelf Sci 39, 529–548.

Chomérat, N., Couté, A., 2008. *Protoperidinium bolmonense* sp. nov. (Peridiniales, Dinophyceae), a small dinoflagellate from a brackish hypereutrophic lagoon (south of France). Phycologia 47, 392–403.

Dai, Y., Yang, S., Zhao, D., Hu, C., Xu, W., Anderson, D.M., Li, Y., Song, X.-P., Boyce, D.G., Gibson, L., Zheng, C., Feng, L., 2023. Coastal phytoplankton blooms expand and intensify in the 21st century. Nature 615. https://doi.org/10.1038/s41586-023-05760-y.

Dale, B., 2009. Eutrophication signals in the sedimentary record of dinoflagellate cysts in coastal waters. J. Sea Res. 61, 103–113.

Diaz, R.J., Rosenberg, R., 2008. Spreading dead zones and consequences for marine ecosystems. Science 321, 926–929.

Doucette, G.J., McGovern, E.R., Babinchak, J.A., 1999. Algicidal bacteria active against *Karenia brevis* (Dinophyceae). I. Bacterial isolation and characterization of killing activity. J. Phycol. 35, 1447–1454.

Eppley, R.W., Harrison, W.G., 1975. Physiological ecology of *Gonyaulax polyedra* a red water dinoflagellate of southern California. In: LoCicero, V.R. (Ed.), Proceedings of the First International Conference of Toxic Dinoflagellate Blooms. Masachusetts Science and Technology Foundation, Wakefield MA, pp. 11–22.

Fernandes, L.D.A., Corte, G.N., Moura, L., Reis, C., Matos, T., Moreno, D., Cortez, P.S.A., de Carvalho, W.F., Monteiro-Ribas, W., Gonçalves, J.E.A., Ribeiro, F., Thomazelli, F., Rizzini-Ansari, N., Neto, E.B.F., Gaelzer, L.R., de Souza Martins, E., Lobão, M.M., Baeta-Neves, M.H., Coutinho, R., 2023. Effects of dredging activities and seasonal variation on coastal plankton assemblages: results from 10 years of environmental monitoring. Environ. Monit. Assess. 195, 261.

Fisher, T.R., Melack, J.M., Grobbelaar, J.U., Howarth, R.W., 1995. Nutrient limitation of phytoplankton and eutrophication of inland, estuarine, and marine waters. In: Tiessen, H. (Ed.), Phosphorus in the Global environment: transfers, Cycles and Management. Wiley and Son, New York, pp. 301–322.

Frehi, H., Couté, A., Mascarell, G., Perrette-Gallet, C., Ayada, M., Kara, M.H., 2007. Dinoflagellés toxiques et/ou responsables de blooms dans la baie d'Annaba (Algérie). C. R. Biologies 330, 615–628 [In French with English Abstract].

Gernez, P., Zoffoli, M.L., Lacour, T., Fariñas, T.H., Navarro, G., Caballero, I., Harmel, T., 2023. The many shades of red tides: sentinel-2 optical types of highly-concentrated harmful algal blooms. Remote Sens. Environ. 287, 113486.

Glibert, P.M., Wilkerson, F.P., Dugdale, R.C., Raven, J.A., Dupont, C.L., Leavitt, P.R., Parker, A.E., Burkholder, J.M., Kana, T.M., 2016. Pluses and minuses of ammonium and nitrate uptake and assimilation by phytoplankton and implications for productivity and community composition, with emphasis on nitrogen-enriched conditions. Limnol. Oceanogr. 61, 165–197.

Gohin, F., Van der Zande, D., Tilstone, G., Eleveld, M.A., Lefebvre, A., Andrieux-Loyer, F., Blauw, A.N., Bryère, P., Devreker, D., Garnesson, P., Hernández Fariñas, T., Lamaury, Y., Lampert, L., Lavigne, H., Menet-Nedelec, F., Pardo, S., Saulquin, B., 2019. Twenty years of satellite and in situ observations of surface chlorophyll-a from the northern Bay of Biscay to the eastern English Channel. Is the water quality improving? Remote Sens. Environ 233, 111343.

Goldstein, M., 2011. San Diego red tide eaten alive by single-celled predator. Deep Sea News. www.deepseanews.com/2011/10/san-diego-red-tide-eaten-alive-bysingle-celled-predator/.

Guillaud, J.F., Aminot, A., Delmas, D., Gohin, F., Lunven, M., Labry, C., Herbland, A., 2008. Seasonal variation of riverine nutrient inputs in the northern Bay of Biscay (France), and patterns of marine phytoplankton response. J. Mar. Syst. 72, 309–319.

Howard, J., 1996. Red tides rising. Scripps Inst. Ocean Explor. 2, 2–9.

Jeong, H.J., Yoo, Y.D., Park, J.Y., Song, J.Y., Song, T.K., Lee, S.H., Kim, K.Y., Yih, W.H., 2005. Feeding by phototrophic red-tide dinoflagellates: five species newly revealed and six species previously known to be mixotrophic. Aquat. Microb. Ecol. 40, 133–150.

Kahru, M., Anderson, C., Barton, A.D., Carter, M.L., Catlett, D., Send, U., Sosik, H.M., Weiss, E.L., Mitchell, B.G., 2021. Satellite detection of dinoflagellate blooms off California by UV reflectance ratios. Elem. Sci. Anth. 9, 1.

Kokinos, J.P., Anderson, D.M., 1995. Morphological development of resting cysts in cultures of the marine dinoflagellate *Lingulodinium polyedrum* (= L. machaerophorum). Palynology 19, 143–166.

Kudela, R.M., Cochlan, W.P., 2000. Nitrogen and carbon uptake kinetics and the influence of irradiance for a red tide bloom off southern California. Aquat. Microb. Ecol. 21, 31–47.

Lambert, C., Penaud, A., Vidal, M., Gandini, C., Labeyrie, L., Chauvaud, L., Erhold, A., 2020. Striking forest revival at the end of the Roman Period in north-western. Europe. Sci. Rep. 10, 21984.

Lambert, C., Penaud, A., Poirier, C., Goubert, E., 2022. Distribution of modern dinocysts in surface sediments of southern Brittany (NW France) in relation to environmental parameters: implications for paleoreconstructions. Rev. Palaeobot. Palynol. 297, 104578.

Larrazabal, M.E., Lassus, P., Maggi, P., Bardouil, M., 1990. Kystes modernes de dinoflagellés en Baie de Vilaine-Bretagne Sud (France). Cryptogamie, Algol. 11, 171–185.

Lassus, P., Chomérat, N., Hess, P., Nézan, E., 2016. Toxic and Harmful Microalgae of theWorld Ocean /Micro-algues toxiques et nuisibles de l'océan mondial. International Society for the Study of Harmful Algae / Intergovernmental Oceanographic Commission of UNESCO, Denmark IOC Manuals and Guides, p. 68 [Bilingual English/French].

Lazure, P., Garnier, V., Dumas, F., Herry, C., Chifflet, M., 2009. Development of a hydrodynamic model of the Bay of Biscay. Validation of hydrology. Cont. Shelf Res. 29 (8), 985–997.

Lazure, P., Jegou, A.-.M., 1998. 3D modelling of seasonal evolution of Loire and Gironde plumes on Biscay Bay continental shelf. Oceanol. Acta 21, 165–177.

Lazure, P., Salomon, J.-.C., 1991. Coupled 2-d and 3-d modeling of coastal hydrodynamics. Oceanol. Acta 14, 173–180.

Lewis, J., 1988. Cysts and sediments: *gonyaulax polyedra* (*Lingulodinium machaerophorum*) in Loch Creran. J. Mar. Biol. Ass. U.K. 68, 701–714.

Lewis, J., Hallett, R., 1997. *Lingulodinium polyedrum* (*Gonyaulax polyedra*) a blooming dinoflagellate. Oceanogr. Mar. Biol. 35, 97–161.

Marasović, I., Vukadin, I., 1982. "Red tide" in the Vranjic basin (Kaštela Bay). Bilješke - Notes. Institut za Oceanografiju i Ribarstvo — Split 1–7.

Marasović, I., Ninčević, Z., Odžak, N., 1995. The effect of temperature on blooms of *Lingulodinium polyedra* and *Alexandrium minutum* in Kastela Bay. In: Lassus, P., Arzul, G., Erard, E., Gentien, P., Marcaillou, C. (Eds.), Harmful Algal Blooms. Lavoisier, Intercept Ltd, pp. 187–192.

Margalef, R., 1956. Estructura y dinámica de la "purga de mar" en la Ría de Vigo. Investigacion Pesquera V 113–134.

Margalef, R., 1978. Life-forms of phytoplankton as survival alternatives in an unstable environment. Oceanolog. Acta 1, 493–509.

Ménesguen, A., Desmit, X., Dulière, V., Lacroix, G., Thouvenin, B., Thieu, V., Dussauze, M., 2018. How to avoid eutrophication in coastal seas? A new approach to derive river-specific combined nitrate and phosphate maximum concentrations. Sci. Total Environ. 628–629, 400–414.

Ménesguen, A., Dussauze, M., 2015. Détermination des "bassins récepteurs" marins des principaux fleuves français de la façade Manche-Atlantique, et de leurs rôles respectifs dans l'eutrophisation phyto-planctonique des masses d'eau DCE et des sous-régions DCSMM. Phase 1 (2013): calcul de scénarios optimaux à partir des "bassins récepteurs". Phase 2 (2014): Simulation de scénarios imposés et des scénarios optimaux. Rapport [In French]. https://archimer.ifremer.fr/doc/00333/44422/.

Ménesguen, A., Dussauze, M., Dumas, F., Thouvenin, B., Garnier, V., Lecornu, F., Répécaud, M., 2019. Ecological model of the Bay of Biscay and English Channel shelf for environmental status assessment part 1: nutrients, phytoplankton and oxygen. Ocean Model 133, 56–78.

Mertens, K.N., Ribeiro, S., Bouimetarhan, I., Caner, H., Combourieu Nebout, N., Dale, B., de Vernal, A., Ellegaard, M., Filipova, M., Godhe, A., Goubert, E., Grøsfjeld, K., Holzwarth, U., Kotthoff, U., Leroy, S.A.G., Londeix, L., Marret, F., Matsuoka, K., Mudie, P.J., Naudts, L., Peña-Manjarrez, J.L., Persson, A., Popescu, S.-.M., Pospelova, V., Sangiorgi, F., van der Meer, M., Vink, A., Zonneveld, K.A.F., Vercauteren, D., Vlassenbroeck, J., Louwye, S., 2009a. Process length variation in cysts of a dinoflagellate, Lingulodinium machaerophorum, in surface sediments: investigating its potential as salinity proxy. Mar. Micropaleont. 70, 54–69.

Mertens, K.N., Verhoeven, K., Verleye, T., Louwye, S., Amorim, A., Ribeiro, S., Deaf, A.S., Harding, I., De Schepper, S., Kodrans-Nsiah, M., de Vernal, A., Radi, T., Dybkjaer, K., Poulsen, N.E., Feist-burkhardt, S., Chitolie, J., González Arango, C., Heilmann-Clausen, C., Londeix, L., Turon, J.-.L., Marret, F., Matthiessen, J., McCarthy, F.M.G., Prasad, V., Pospelova, V., Kyffin Hughes, J.E., Riding, J.B., Rochon, A., Sangiorgi, F., Welters, N., Sinclair, N., Thun, C., Soliman, A., Van Nieuwenhove, N., Vink, A., Young, M., 2009b. Determining the absolute abundance of dinoflagellate cysts in recent marine sediments: the *Lycopodium* marker-grain method put to the test. Rev. Palaeobot. Palynol. 157, 238–252.

Mertens, K.N., Carbonell-Moore, M.C., Pospelova, V., Head, M.J., Highfield, A., Schroeder, D., Gu, H., Andre, K.B., Fernandez, M., Yamaguchi, A., Takano, Y., Matsuoka, K., Nézan, E., Bilien, G., Okolodkov, Y., Koike, K., Hoppenrath, M., Pfaff, M., Pitcher, G., Al-Muftah, A., Rochon, A., Lim, P.T., Leaw, C.P., Lim, Z.F., Ellegaard, M., 2018. Pentaplacodinium saltonense gen. et sp. nov. (Dinophyceae) and its relationship to the cyst-defined genus Operculodinium and yessotoxin-producing Protoceratium reticulatum. Harmf. Algae 77, 57–77.

Mertens, K.N., Morquecho, L., Carbonell-Moore, C., Meyvisch, P., Gu, H., Bilien, G., Duval, A., Derrien, A., Pospelova, V., Śliwińska, K.K., Gárate-Lizárraga, I., Pérez-Cruz, B., 2023. *Pentaplacodinium lapazense* sp. nov. from Central and Southern Gulf of California, a new non-toxic gonyaulacalean resembling *Protoceratium reticulatum*. Mar. Micropaleontol. 178, 102187.

Morton, S.L., Vershinin, A., Leighfield, T.A., Smith, L., Quilliam, M., 2007. Identification of yessotoxin in mussels from the Caucasian Black Sea Coast of the Russian Federation. Toxicon 50, 581–584.

Neaud-Masson, N., Lemoine, M., Daniel, A., 2023. Procédure nationale pour la mise en œuvre du réseau d'observation et de surveillance du phytoplancton et de l'hydrologie dans les eaux littorales (REPHY). Document de prescriptions. Version 2 de janvier 2023. ODE/VIGIES/23-01. https://doi.org/10.13155/50389 [In French].

Paulmier, G., 1965. Le microplancton de la rivière d'Auray. Rev. Trav. Inst. Pêches marit. 29, 211–224.

Paulmier, G., 1972. Seston-phytoplancton et microphytobenthos en rivière d'Auray. Leur Rôle Dans Le Cycle Biologique Des Huîtres (Ostrea Edulis L.). Thèse Doct. Univ. Sci. Univ. Marseille Saint-Charles, p. 142.

Paulmier, G., 1994. Les dinophycées pelagiques et benthiques du Golfe de Gascogne Sud de la Bretagne à Arcachon. Annales de la société des sciences naturelles de la Charente-Maritime VIII 289–357.

Paz, B., Riobó, P., Fernández, A.L., Fraga, S., Franco, J.M., 2004. Production and release of yessotoxins by the dinoflagellates *Protoceratium reticulatum* and *Lingulodinium polyedrum* in culture. Toxicon 44, 251–258.

Paz, B., Daranas, A.H., Norte, M., Riobó, P., Franco, J.M., Fernández, J.J., 2008. Yessotoxins, a group of marine polyether toxins: an overview. Mar. Drugs 6, 73–102.

Peña-Manjarrez, J.L., Helenes, J., Gaxiola-Castro, G., Orellana-Cepeda, E., 2005. Dinoflagellate cysts and bloom events at Todos Santos Bay, Baja California, México, 1999–2000. Cont. Shelf Res. 25, 1375–1393.

Pfiester, L.A., Anderson, D.M., 1987. Chapter 14. Dinoflagellate life-cycles and their environmental control (editor). In: Taylor, F.J.R. (Ed.), The Biology of Dinoflagellates. Botanical Monographs. Blackwell Scientific Publications, Oxford, pp. 611–648. Volume 21.

Pitcher, G.C., Foord, C.J., Macey, B.M., Mansfield, L., Mouton, A., Smith, M.E., Osmond, S.J., van der Molen, L., 2019. Devastating farmed abalone mortalities attributed to yessotoxin-producing dinoflagellates. Harmf. Algae 81, 30–41.

Prevett, A., Lindström, J., Xu, J., Karlson, B., Selander, E., 2019. Grazer-induced bioluminescence gives dinoflagellates a competitive edge. Curr. Biol. 29, R551–R567.

Prézelin, B.B., Matlick, H.A., 1983. Nutrient-dependent low-light adaptation in the dinoflagellate *Gonyaulax polyedra*. Mar. Biol. 74, 141–150.

Puillat, I., Lazure, P., Jégou, A.M., Lampert, L., Miller, P.I., 2004. Hydrographical variability on the French continental shelf in the Bay of Biscay, during the 1990s. Cont. Shelf Res. 24 (10), 1143–1163.

Ralston, D.K., Brosnahan, M.L., Fox, S.E., Lee, K.D., Anderson, D.M., 2015. Temperature and residence time controls on an estuarine harmful algal bloom: modeling hydrodynamics and *Alexandrium catenella* in Nauset Estuary. Estuaries Coast 38, 2240–2258.

Ratmaya, W., Soudant, D., Salmon-Monviola, J., Plus, M., Cochennec-Laureau, N., Goubert, E., Andrieux-Loyer, F., Barillé, L., Souchu, P., 2019. Reduced phosphorus loads from the Loire and Vilaine rivers were accompanied by increasing eutrophication in the Vilaine Bay (south Brittany, France). Biogeosciences 16, 1361–1380.

Ratmaya, W., Laverman, A.M., Rabouille, C., Akbarzadeh, Z., Andrieux-Loyer, F., Barillé, L., Barillé, A.-.L., Le Merrer, Y., Souchu, P., 2022. Temporal and spatial variations in benthic nitrogen cycling in a temperate macro-tidal coastal ecosystem: observation and modeling. Cont. Shelf Res. 235, 104649.

Reish, D.J., 1963. Mass mortality of marine organisms attributed to the "red tide" in Southern California. Calif. Fish and Game 49, 165–170.

REPHY, 2022. REPHY dataset - French Observation and Monitoring program for Phytoplankton and Hydrology in coastal waters. Metropolitan Data. SEANOE. https://doi.org/10.17882/47248.

REPHYTOX, 2022. REPHYTOX dataset. French Monitoring program for Phycotoxins in marine organisms. Data since 1987. https://www.seanoe.org/data/00361/47251/.

Retho, M., Quemener, L., Le Gall, C., Repecaud, M., Souchu, P., Gabellec, R., Manach, S., 2022. COAST-HF - data and metadata from the MOLIT buoy in the Vilaine Bay. SEANOE. https://doi.org/10.17882/46529.

Rosenberg, R., Hellman, B., Johansson, B., 1991. Hypoxic tolerance of marine benthic fauna. Mar. Ecol. Prog. Ser. 79, 127–131.

Roux, P., Siano, R., Souchu, P., Collin, K., Schmitt, A., Manach, S., Retho, M., Pierre-Duplessix, O., Marchand, L., Colliec-Jouault, S., Pochic, V., Zoffoli, M.L., Gernez, P., Schapira, M., 2022. Spatio-temporal dynamics and biogeochemical properties of green seawater discolorations caused by the marine dinoflagellate *Lepidodinium chlorophorum* along southern Brittany coast. Estuar. Coast. Shelf Sci. 275, 107950.

Roux, P., Schapira, M., Mertens, K.N., André, C., Terre-Terrillon, A., Schmitt, A., Manach, S., Collin, K., Serghine, J., Noel, C., Siano, R., 2023. When phytoplankton does not bloom: the case of the dinoflagellate *Lepidodinium chlorophorum* in southern Brittany (France) assessed by environmental DNA. Prog. Oceanogr. https://doi.org/10.1016/j.pocean.2023.102999.

Rubini, S., Albonetti, S., Menotta, S., Cervo, A., Callegari, E., Cangini, M., Dall'Ara, S., Baldini, E., Vertuani, S., Manfredini, S., 2021. New trends in the occurrence of yessotoxins in the Northwestern Adriatic Sea. Toxins (Basel) 13, 634.

Ruiz-de la Torre, M.C., Maske, H., Ochoa, J., Almeda-Jauregui, C.O., 2013. Maintenance of coastal surface blooms by surface temperature stratification and wind drift. PLoS One 8, e58958. https://doi.org/10.1371/journal.pone.0058958.

Sacilotto Detoni, A.M., Navarro, G., Garrido, J.L., Rodríguez, F., Hernández-Urcera, J., Caballero, I., 2023. Mapping dinoflagellate blooms (*Noctiluca* and *Alexandrium*) in aquaculture production areas in the NW Iberian Peninsulawith the Sentinel-2/3 satellites. Sci. Total Environ. 868, 161579.

Schapira, M., Roux, P., Andre, C., Mertens, K., Bilien, G., Terre Terrillon, A., Le Gac-Abernot, C., Siano, R., Quere, J., Bizzozero, L., Bonneau, F., Bouget, J.-.F., Cochennec-Laureau, N., Collin, K., Fortune, M., Gabellec, R., Le Merrer, Y., Manach, S., Pierre-Duplessix, O., Retho, M., Schmitt, A., Souchu, P., Stachowski-Haberkorn, S., 2021. Les Efflorescences de *Lepidodinium chlorophorum* au large de la Loire et de la Vilaine: déterminisme et conséquences sur la qualité des masses d'eau côtières. Projet EPICE – Rapport final. RST/LER/MPL/21.10. https://archimer.ifremer.fr/doc/00724/83598/.

Siano, R., Chapelle, A., Antoine, V., Michel-Guillou, E., Rigaut-Jalabert, F., Guillou, L., Hégaret, H., Leynaert, A., Curd, A., 2020. Citizen participation in monitoring phytoplankton seawater discolorations. Mar. Policy 117, 103039.

Smayda, T.J., 2002. Turbulence, watermass stratification and harmful algal blooms: an alternative view and frontal zones as "pelagic seed banks. Harmf. Algae 1, 95–112. https://doi.org/10.1016/S1568-9883(02)00010-0.

Smith, M.E., Robertson, L., Bernard, L.S., 2018. An optimized Chlorophyll a switching algorithm for MERIS and OLCI in phytoplankton-dominated waters. Remote Sens. Environ. 215, 217–227.

Souchu, P., Cochennec-Laureau, N., Ratmaya, W., Retho, M., Andrieux, F., Le Merrer, Y., Barillé, L., Barillé, A.-.L., Goubert, E., Plus, M., Laverman, A., 2018. Diagnostic étendu de l'eutrophisation (DIETE). Rôle des sédiments dans le cycle des nutriments et impacts sur l'eutrophisation de la baie de Vilaine (2014–2017). Rapport de contrat. RST/LER/MPL/18.04.

Sournia, A., Belin, C., Billard, C., Erard-Le Denn, E., Fresnel, J., Lassus, P., Pastoureau, A., Soulard, R., 1992. The repetitive and expanding occurrence of green, bloom-forming dinoflagellate (Dinophyceae) on the coasts of France. Cryptogam. Algol. 13, 1–13.

Stobo, L.A., Lewis, J., Quilliam, M.A., Hardstaff, W.R., Gallacher, S., Webster, L., Smith, E., McKenzie, M., 2003. Detection of yessotoxin in UK and Canadian isolates of phytoplankton and optimization and validation of LC-MS methods. In: Bates, S. (Ed.), Proceedings of the eighth Canadian workshop on harmful marine algae Can. Tech. Rep. Fish. Aquat. Sci. 2498, 8–14.

Stohler, R., 1959. The red tide of 1958 at Ensenada, Baja California, Mexico. Veliger 2, 32–35.

Terenko, G., Krakhmalny, A., 2021. Red tide of *Lingulodinium polyedrum* (Dinophyceae) in Odesa Bay. Turk. J. Fish. & Aquat. Sci. 22. TRJFAS20312.

Tillmann, U., Bantle, A., Krock, B., Elbrächter, M., Gottschling, M., 2021. Recommendations for epitypification of dinophytes exemplified by *Lingulodinium polyedra* and molecular phylogenetics of the Gonyaulacales based on curated rRNA sequence data. Harmf. Algae 104, 101956.

Tubaro, A., Sidari, L., Della Loggia, R., Yasumoto, T., 1998. Occurrence of homoyessotoxin in phytoplankton and mussels from Northern Adriatic Sea. In: Reguera, B., Blanco, J., Fernández, M.L., Wyatt, T. (Eds.), Harmful Algae. Xunta de Galicia and Intergovernmental Oceanographic Commission of UNESCO. Santiago de Compostela, Grafisant, pp. 470–472.

Utermöhl, H., 1958. Zur vervollkommnung der quantitativen phytoplankton methodik. Mitt. - Int. Ver. Theor. Angew. Limnol. 9, 1–38.

Van Heukelem, L., Thomas, C.S., 2001. Computer-assisted high-performance liquid chromatography method development with applications to the isolation and analysis of phytoplankton pigments. J. Chromatogr. A 910, 31–49.

Van Nieuwenhove, N., Head, M.J., Limoges, A., Pospelova, V., Mertens, K.N., Matthiessen, J., De Schepper, S., de Vernal, A., Eynaud, F., Londeix, L., Marret, F., Penaud, A., Radi, T., Rochon, A., 2020. An overview and brief description of common marine organic-walled dinoflagellate cyst taxa occurring in surface sediments of the Northern Hemisphere. Mar. Micropaleont. 159, 101814.

Velo-Suárez, L., Brosnahan, M.L., Anderson, D.M., McGillicuddy Jr., D.J., 2013. A quantitative assessment of the role of the parasite amoebophrya in the termination of *Alexandrium fundyense* blooms within a small coastal embayment. PLoS One 8, e81150. https://doi.org/10.1371/journal.pone.0081150.

Wang, Z.-.H., Qi, Y.-.Z., Yang, Y.-.F., 2007. Cyst formation: an important mechanism for the termination of *Scrippsiella trochoidea* (Dinophyceae) bloom. J. Plankton Res. 29, 209–218.

Zapata, M., Fraga, S., Rodríguez, F., Garrido, J.L., 2012. Pigment-based chloroplast types in dinoflagellates. Mar. Ecol. Prog. Ser. 465, 33–52.

Zonneveld, K.A.F., Marret, F., Versteegh, G.J.M., Bogus, K., Bonnet, S., Bouimetarhan, I., Crouch, E., et al., 2013. Atlas of modern dinoflagellate cyst distribution based on 2405 data points. Rev. Palaeobot. Palynol. 191, 1–197.